STUDIES OF SHIP MANEUVERING
"Response to Propeller and Rudder Actions"

by C. Lincoln Crane, Jr. - SNAME Associate Member
Research Engineer, Davidson Laboratory
Stevens Institute of Technology, Hoboken, New Jersey;
presently Marine Designer, Tanker Department
Esso International, Inc., New York, New York

ABSTRACT

An attempt is made to extend ship-maneuvering analysis for application at low ship speeds. Captive-model experiments are made to investigate effects of non-equilibrium propeller speeds on rudder force and effective thrust. Other experiments are made to explore first-order effects of very large drift angles and pure yaw rotation on hull hydrodynamic reactions. The experimental results, together with previous rotating-arm data, are applied in motion equations, accounting for both extreme propeller actions and the occurrence of large drift angles and turning rates. Also included are propulsion and rudder time lags, and the influence of uniform water current on ship trajectory. The equations are programmed for computation, and ship response to a simple docking maneuver is predicted. The computation is repeated several times to examine sensitivity of ship motions and trajectory to variations of operating parameters, namely, maximum reverse propeller speed, engine response time, and water-current direction.

INTRODUCTION

Upon entering pilot waters from seaward, a ship's control problems change, in nature, becoming increasingly difficult until maneuvers are concluded (successfully or otherwise) at dockside, anchorage, or mooring. Throughout this period, control of ship's trajectory and speed must be sufficient to assure safe passage through channels, bridges, and locks; and to avoid collisions with other vessels.

Unfortunately, when danger of collision or grounding is greatest, a speed otherwise "prudent" for navigation can be too slow for adequate directional control. This is because steady hydrodynamic forces depend on the square of ship speed, while external disturbances do not. A reduction to one-quarter speed, for example, will cut rudder force to one-sixteenth, but will not diminish the adverse effects of wind and current.

Other ship characteristics contribute to the problem. First, rudder forces of a single-screw ship depend heavily on propeller speed. Second, large merchant ships have small thrust-to-mass ratios, hence they respond sluggishly to propeller actions. And third, lightly loaded merchant ships have large ratios of above-water to below-water surface area, causing wind effects to be accentuated.

These factors combine to cause frequent saturation of propeller and rudder forces. Sometimes control is quite inadequate. Then, auxiliary forces such as tugs, bow-thruster, or anchor must be called upon.

The simplified motion equations used in most studies of ship control provide satisfactory predictions of maneuvers under cruising (constant throttle) conditions, but are not sufficiently general to treat many real control problems, such as those which occur at low ship speeds.

Controllability surveys by Norrbin,[1] Eda and Crane,[2] Williams and Noble,[3] Goodman,[4] and Abkowitz[5] discuss the usual forms of equations and their solutions. None include propeller-speed changes, wind force, or water-current effect. Saunders,[6] and more recently Hawkins,[7] have discussed special low-speed maneuvers without using equations of motion. Crane, Uram[8] and Chey[8] have formulated motion equations for mooring and docking maneuvers of a destroyer and a submarine. But most efforts on non-equilibrium propeller effects have concentrated on ship-stopping. These works are summarized in Reference 9. Papers By English,[10] Hawkins, Stuntz and Taylor,[11] and others treat bow-thrusters and other maneuvering-propulsion

devices (MPD) but these do not include MPD forces in maneuvering analyses.

The present work is an attempt to extend the generality of ship-maneuvering analysis to include engine-maneuver and water-current effects and introduce the possibilities of very large drift angles and space turning rates. Equations of motion are formulated for translation and rotation of a surface ship maneuvering in a reference frame which is fixed with respect to a moving water mass (the water current). The independent ship variables comprise propeller speed and rudder angle. The equations are solved with respect to the coordinate frame moving with the water, and the solution is transformed to a fixed coordinate frame. Resultant ship velocity is integrated to obtain ship's position and orientation at any time. Water current is a parameter, and is made zero when discussing other effects.

Coefficients of the equations are obtained from experiment, calculation, and existing data. Strong couplings among ship speed, propeller speed, and rudder angle (at maneuvering speeds) are investigated by captive-model tests on straight path in a towing tank. Indications of hydrodynamic reactions to very large drift angles and to pure yaw rotation are obtained experimentally. Numerical integrations are performed by digital computer.

A few examples of computed maneuvers are given to illustrate uses which can be made of more general analyses of ship maneuvering. Using the computation procedure developed, the sensitivity of ship response to particular ship parameters is studied for a simple ship-docking maneuver.

This project was sponsored by the Bureau of Ships General Hydromechanics Research Program under Contract Nonr 263(63) and technically administered by the David Taylor Model Basin.

EQUATIONS OF MOTION - GENERAL

General Form of Motion Equations

Differential equations describing the motion of a ship are written with respect to a reference frame rotating with the ship's axes, the origin of which is chosen coincident with the ship's center of mass (see Figure 1, following page).

$$\vec{F} = m\left(\frac{d\vec{V}}{dt} + \vec{\omega} \times \vec{V}\right) \qquad \vec{N} = I\frac{d\vec{\omega}}{dt} + \vec{\omega} \times I\,\vec{\omega} \tag{1}$$

where $\vec{F}$ sum of all external forces acting

$\vec{N}$ sum of all external moments acting

$\vec{V}$ velocity of ship center-of-mass relative to the water

$\vec{\omega}$ angular velocity of ship (ship's axes)

I ship inertia tensor

All vectors can be expressed in rotating (ship axes) coordinates. For a surface ship in calm water, these vector equations are reduced to three Cartesian equations by applying the following simplifying assumptions:

1. Ship is constrained to move in its lateral plane (i.e., the x,y-plane), which is horizontal.
2. Center of mass is in the principal plane of symmetry of the hull.
3. Mass and center of mass are constant.
4. Products of inertia are zero.

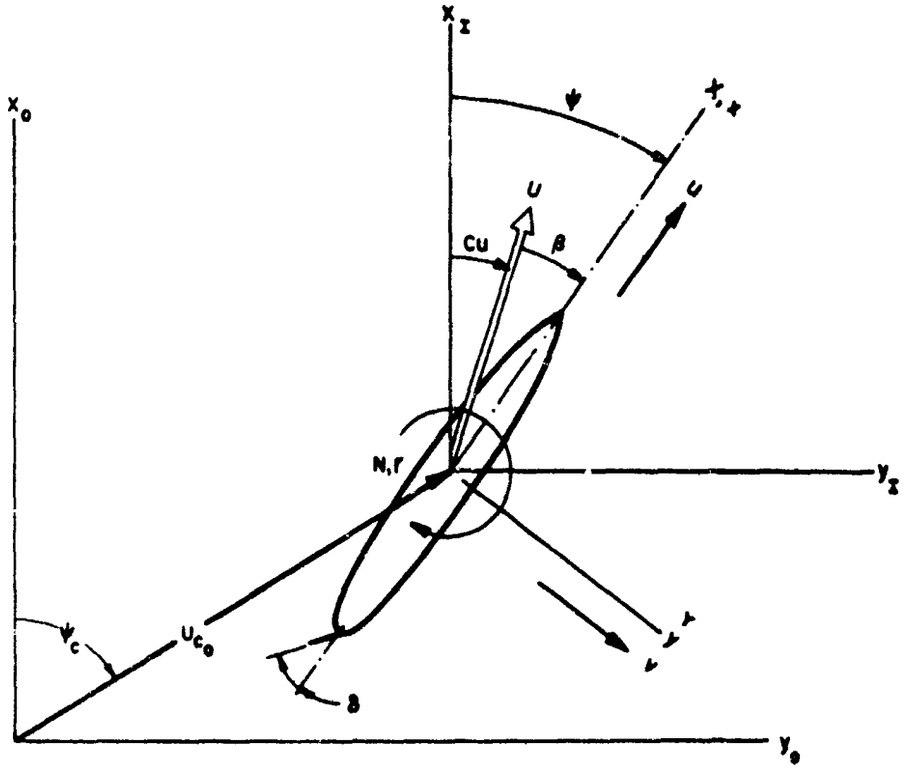

FIGURE I. REFERENCE FRAMES

Then,

$$m(\dot{u} - rv) = X \qquad m(\dot{v} + ru) = Y \qquad I_z\dot{r} = N \tag{2}$$

where X and Y represent summations of unbalanced external forces acting in the x and y directions, and N the summation of unbalanced moments about the z-axis.

External forces arise from hydrodynamic reactions to hull motion, propeller and rudder actions, aerodynamic reactions on hull structure, and all other forces which may be applied by waves, bow-thruster, anchor chain, tugboat, mooring lines, etc. In this analysis, only hull hydrodynamic and propeller-rudder forces are included. In succeeding sections, their contributions to X, Y, and N are considered.

Reference Frames

It is usually desirable to describe low-speed maneuvers relative to an inertial reference frame fixed in the earth. However, the motion equations and solution are greatly simplified if referred to a coordinate frame fixed in the ship,* with subsequent transformation of solutions to the desired reference frame (Figure 1).

With a uniform water current, an additional (intermediate) reference frame is useful. The additional frame maintains the same orientation as the fixed frame, but moves with the steady velocity of the uniform water current. In computation, the first transformation of the solution is from ship axes to intermediate axes. The second transformation simply adds the water-current velocity components, to obtain motions relative to the final desired reference frame.

It is emphasized that the uniform water current need not enter the differential equations of motion, because a steady velocity will introduce no acceleration in the motion equations. The current is entirely accounted for in the final integration of velocities. Steps involved in the velocity transformations are shown below.

(1) Ship velocity components (expressed in ship axes) are transformed to intermediate axes by a rotation of coordinates.

$$\begin{aligned} u_I &= u\cos\psi - v\sin\psi \\ v_I &= u\sin\psi + v\cos\psi \end{aligned} \tag{3}$$

and

$$\psi = \int_0^t r\,dt + \psi(0)$$

where u and v are coordinates of velocity along ship axes, and u_I and v_I are components of ship velocity along intermediate axes.

(2) Components of water-current velocity are then added to obtain ship motion relative to fixed inertial axes.

$$\begin{aligned} u_O &= u\cos\psi - v\sin\psi + U_{c_O}\cos\psi_c \\ v_O &= u\sin\psi + v\cos\psi + U_{c_O}\sin\psi_c \end{aligned} \tag{4}$$

---

*Orientation of ship axes with respect to ship geometry varies according to ship loading conditions because, for convenience, x and y ship axes are taken horizontal (hence, z-axis vertical).

keeping in mind that the intermediate axes (I) and fixed inertial axes (o) are parallel.

Time integration of the velocities u_o and v_o yields instantaneous ship position (x_o, y_o) with respect to any chosen origin.

HULL CONTRIBUTIONS TO EXTERNAL FORCE AND MOMENT

Hydrodynamic forces exerted on a ship's hull are attributed to viscous and inertial fluid effects which are expressed as functions of hull motions and accelerations. Since a wide range of maneuvering motions may occur at low ship speeds, hydrodynamic representations are separated according to application to cruising-type or docking-type maneuvers. The former case is considered first.

A convenient form for expressing hull hydrodynamic forces is available in the Taylor series expansion.[12] In the present analysis, the general expansion is specialized to the surge, sway, and yaw motions of a ship.

The following simplifications, additional to those noted in the previous section, are made:

1. The hydrodynamic derivative coefficients X'_{vv}, X'_{rr}, $Y'_{\dot{r}}$, and $N'_{\dot{v}}$ are assumed to be negligible. For convenience, a term proportional to uU is used to account for X'_o and drift-angle effects.
2. Hydrodynamic terms of order four and higher are assumed to be negligible.
3. Forces due to hull motions and accelerations are represented to be independent of propeller and rudder actions.
4. The ship floats in deep ($D/H \sim 3.5$), calm, unrestricted water.

Simplification (3) is necessary because of the absence of captive-model experimental data for a ship on curved path with reversed propeller rotation, or in any propeller condition far removed from model or ship self-propulsion point. An indication of the effects of non-equilibrium propeller speed on hull hydrodynamic data was obtained by inspection of rotating-arm test results for a model of T.S. EMPIRE STATE IV.[13] The measured effects cannot be explained simply on the basis of propeller-side-force changes at different propeller loadings. Although the differences are large enough to warrant further investigation, they are of second-order importance for present purposes.

With the preceding simplifications, the non-linear hull force-and-moment expressions, retaining third-order terms in the velocities, may be written as

$$\left.\begin{aligned} X_{hull} &= A_o\dot{u} + A_1uU + A_2rv \\ Y_{hull} &= B_o\dot{v} + B_1uv + B_2ur + B_3rv^2/u + B_4r^2v/u + B_5r^3/u + B_6v^3/u \\ N_{hull} &= C_o\dot{r} + C_1uv + C_2ur + C_3rv^2/u + C_4r^2v/u + C_5r^3/u + C_6v^3/u \end{aligned}\right\} \qquad (5)$$

$$A_o = \frac{\rho}{2}L^3HX'_{\dot{u}} \qquad B_o = \frac{\rho}{2}L^3HY'_{\dot{v}} \qquad C_o = \frac{\rho}{2}L^4HN'_{\dot{r}}$$

$$A_1 = \frac{\rho}{2}LHX'_o \qquad B_1 = \frac{\rho}{2}LHY'_v \qquad C_1 = \frac{\rho}{2}L^2HN'_v$$

$$A_2 = \frac{\rho}{2}L^2HX'_{rv} \qquad B_2 = \frac{\rho}{2}L^2HY'_r \qquad C_2 = \frac{\rho}{2}L^3HN'_r$$

$$B_3 = \frac{\rho}{4} L^2 H(Y'_{rvv} + Y'_r) \qquad C_3 = \frac{\rho}{4} L^3 H(N'_{rvv} + N'_r)$$

$$B_4 = \frac{\rho}{4} L^3 H Y'_{rrv} \qquad C_4 = \frac{\rho}{4} L^4 H N'_{rrv}$$

$$B_5 = \frac{\rho}{12} L^4 H Y'_{rrr} \qquad C_5 = \frac{\rho}{12} L^5 H N'_{rrr}$$

$$B_6 = \frac{\rho}{12} LH(Y'_{vvv} + 3Y'_v) \qquad C_6 = \frac{\rho}{12} L^2 H(N'_{vvv} + 3N'_v)$$

All dimensionless coefficients except $X'_{\dot{u}}$, X'_{vr}, $Y'_{\dot{v}}$, and $N'_{\dot{r}}$ are evaluated experimentally, as described in Reference 13.

The derivatives $X'_{\dot{u}}$, $Y'_{\dot{v}}$, and $N'_{\dot{r}}$ relate hydrodynamic forces to body accelerations, and X'_{vr} is taken equal in magnitude to $Y'_{\dot{v}}$. The $Y'_{\dot{v}}$ and $N'_{\dot{r}}$ coefficients are computed following the method of Lewis[14] and Prohaska.[15] For example,

$$Y_{\dot{v}}/m = \frac{\frac{1}{2}\pi K_c \int_{x_b}^{x_s} k_x(x) H^2 dx}{\int_{x_b}^{x_s} S(x) dx}$$

In this stripwise integration, k_x is the two-dimensional lateral added-mass coefficient. This is determined for shiplike sections, by using Prohaska's results. The k_c is a three-dimensional correction factor determined by comparing the exact added-mass computation of the prolate spheroid given by Lamb with that obtained by the stripwise computation for the same spheroid. Factor $S(x)$ is the local sectional area. The rotary acceleration derivative $N'_{\dot{r}}$ is obtained in a similar manner, but includes an x^2 factor in the integrand of the numerator. The longitudinal acceleration derivative $X'_{\dot{u}}$ is taken equal to that of an equivalent prolate spheroid.

Conditions at Very Low Speeds

Experience shows that at moderate ship speeds, drift angle, β, does not normally exceed approximately ±10 degrees, and dimensionless turning rate, r', is normally limited to about 0.7 (corresponding to turning-diameter/ship-length ≈ 3). However, a ship maneuvering at very low speeds may develop much larger drift angles and space turning rates.

Consider the definition of β, as forward speed u becomes small with respect to lateral speed, v:

$$\lim_{u \to 0} \beta = \lim_{u \to 0} \left[-\tan^{-1}\left(\frac{v}{u}\right) \right] = \pm \pi/2$$

In similar fashion, space turning rate grows large as ship speed vanishes; i.e.,

$$\lim_{U \to 0} r' = \lim_{U \to 0} \frac{rL}{U} \to \infty$$

Such situations arise with the action of external forces which are not wholly dependent on ship motions.

Two broad categories of maneuvers are defined:

1. Cruising-type maneuvers: Both of the below criteria are satisfied.

2. Docking-type maneuvers: One or the other of the below criteria is not satisfied.

$$|\beta| < \beta_L \qquad\qquad |r'| < r_L'$$

The above definitions are useful in defining maneuvers for which conventional hydrodynamic expansions are valid. These are called cruising-type maneuvers, and it is for these that most experimental data are obtained. Ranges of variables may be extended to cover docking-type maneuvers, of course (given sufficient data), but it is possible that an expansion other than Taylor's series may be more convenient for treating docking-type maneuvers (double Fourier series, for example). If a Taylor series is used, an expansion point at ($u=v=r=\dot{u}=\dot{v}=\dot{r}=0$) might prove more convenient than at ($u=u_o$, $v=r=\dot{u}=\dot{v}=\dot{r}=0$).

In this paper an example of a simple docking maneuver is computed. The maneuver is terminated as forward motion stops after sustained reversed propeller action. The computation will show a tendency for the ship to develop large values of β and r' at the end of the maneuver. To allow for this, terms exhibiting first-order qualities of the true (steady-state) hydrodynamic reactions are used in this region. Coefficients of the simplified terms are relatively easy to evaluate, since they represent uncoupled drift-angle and yaw-rate effects. The acceleration dependent terms appear as before. Simplifications 3 and 4 still apply.

$$\begin{aligned} X_{hull} &= A_o\dot{u} + A_1 vU + A_2 rv \\ Y_{hull} &= B_o\dot{v} + B_7 vU + B_8\, v\,|v| + B_9 ur \\ N_{hull} &= C_o\dot{r} + C_7 vu + C_8 \frac{vu}{U^2}\,|vu| + C_9\, r\,|r| \end{aligned} \tag{6}$$

The relative importance of steady-state hydrodynamic forces obviously declines (relative to inertia effects) as ship speed decreases. However, it cannot simply be stated that steady-state terms are negligible below any particular speed (except under very special conditions). For example, consider ship response to a pure applied yaw moment. After initial yaw acceleration, the resisting hydrodynamic moment is almost entirely a steady-state damping effect. If steady-state terms were arbitrarily excluded, acceleration without limit would be computed.

PROPELLER AND RUDDER CONTRIBUTIONS TO EXTERNAL FORCE AND MOMENT

An important departure from usual maneuvering analyses, at low ship speeds, is the loss of proportionality between control forces and the hull forces which are associated with motion through the water. The control forces of propeller and rudder can be disproportionately large or small, according to the action of the propeller. External forces and moments attributed to propeller and rudder actions depend on several factors, including—

1. Propeller, hull, and rudder configurations
2. Propeller speed of rotation and angular acceleration
3. Ship linear and angular velocity
4. Rudder angular deflection and deflection rate
5. State of cavitation or ventilation of propeller and rudder
6. Ship hydrodynamic environment, i.e., water density, depth, and lateral boundaries, and waves

The following assumptions, together with those in previous sections, simplify representations of propeller and rudder forces:

1. Ship speed is low, hence lateral ship velocity is small.

2. Yaw rotation is slow.

3. Based on (1) and (2), the lateral component of inflow to propeller and rudder is small.

4. Rudder deflection rate is slow, conforming to normal ship practice (2-1/2°/sec). Also, frequency of rudder oscillation is low; hence errors due to quasi-steady representation are small.

5. Accelerations of propeller rotation, rudder deflection, and hull motion which might affect propeller and rudder forces have negligibly small effects on integrated hull motions.

6. Propeller and rudder are not cavitating appreciably.

With the above assumptions, propeller and rudder forces are represented as functions of propeller speed, n, ship's longitudinal speed, u, and rudder angular deflection, δ.

X Force Due to Propeller and Rudder

The dimensionless thrust coefficient, $k_t = \text{thrust}/\rho d^4 n^2$, is commonly used to represent propeller test results for various conditions of ship speed and propeller rotation. This concept is useful as an aid in understanding and representing propeller force effects. In this study, self-propelled captive-model tests have been used to measure a quantity which will be denoted X (propeller + rudder). This quantity is defined as total measured axial force, $X(u,n,\delta)$, minus the resistance of the model hull without propeller, $X(u,\_\_,\_\_)$. From this, a dimensionless "effective thrust" coefficient is defined.

$$k_x = \frac{X\ (\text{propeller + rudder})}{\rho d^4 n^2} \tag{7}$$

As with open-water propeller thrust characteristics, it is convenient to graph k_x as a function of propeller advance ratio, $J_s = u/nd$, using ship's speed of advance. For clarity, rudder effects are omitted from the next discussion.

Sketch I shows the relation of k_x to J_s in regions of propeller operation which are important for ship-stopping.

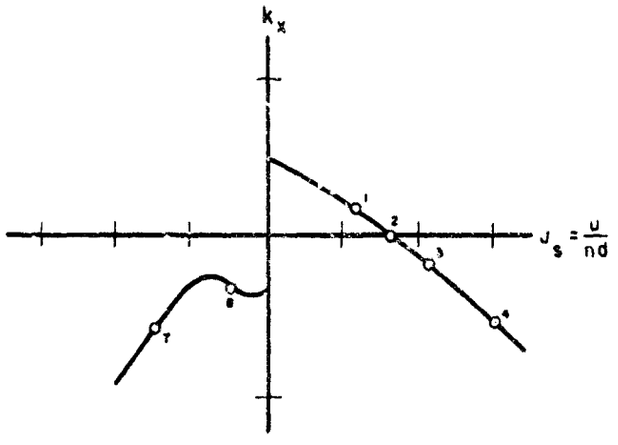

SKETCH I

The path of k_x during rapid propeller reversal is traced:

1. Initial equilibrium condition (thrust = resistance)
2. Propeller speed reduced; blade sections approach zero angle of attack (thrust zero)
3. Propeller speed further reduced; blade sections at negative angles of attack (thrust negative)
4. Propeller speed further reduced; flow about blades completely separates (propeller dragging)
5. Propeller stopped and dragging ...
6. Propeller turning slowly astern but dragging
7. Astern propeller speed increased (blades recover from stall and begin thrusting astern)
8. Propeller speed approaches a constant value; ship speed gradually reduces; astern thrust determined by propeller characteristics

The representation of Sketch I is not useful in the interval between 4 and 7. Mathematically, as n approaches zero, J_s tends to infinity. Furthermore, beyond the blade stall-point at large negative angles of attack, k cannot be represented simply in terms of J_s. For cargo ships and tankers the negative blade-angle stall will occur at a J_s value between 2 and 4. Another dimensionless coefficient is then convenient for expressing "effective propeller thrust." This is the coefficient $c_x = X/\rho d^2 u^2$, used by Bindel[1] and others. The singularity in $J_s = u/nd$ is avoided by using the reciprocal, nd/u.

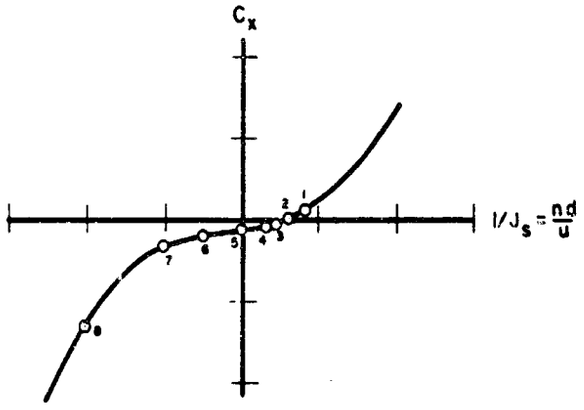

SKETCH II

The characteristic behavior of c_x in a ship-stopping maneuver is shown in Sketch II (numbers correspond to those of Sketch I). Because propeller speed will change much more quickly than ship speed, the behavior of X (propeller) is similar to that of c_x in Sketch II.

Because of slow propeller speeds in the region from 4 to 6, experimental evaluation of c_x is subject to serious scale effect (especially for the propeller operating behind the ship); but if c_x passes from 4 to 6 in a few seconds, the accuracy of the representation in this region is not crucial. An estimated propeller drag coefficient is therefore used (see Appendix A). When unstalled propeller operation resumes (with reversed propeller speed), the k_x vs. J_s relation is again effective and simple to use.

The required segments of the k_x, J_s curve are easily described by simple polynomials in J_s. For example, in the region from 1 to 4 (of Sketch I), an adequate curve fit is obtained with $k_x = a_0 + a_1 J_s + a_2 J_s^2$. And since

$$X \text{ (propeller)} = k_x \rho d^4 n^2$$

substitution of the polynomial in J_s for k_x, and $\frac{u}{nd}$ for J_s, yields

$$X \text{ (propeller)} = (\rho d^4 a_o) n^2 + (\rho d^3 a_1) un + (\rho d^2 a_2) u^2 \qquad (8)$$

where a_o, a_1, a_2 are determined for a particular propeller and hull.

In similar fashion, the k_x curve segment passing from point 7 through point 8 may be curve fitted to J_s. For digital computation of maneuvers, the correct expression for k_x can be automatically selected according to the instantaneous value of J_s, in accordance with rules based on Sketch I.

Rudder effect on X force is treated next. The drag of a rudder mounted aft of an ahead-turning propeller is a function of rudder angle, ship speed, and propeller speed. If k_x is approximately parabolic with rudder angle, δ, a simple extension of the propeller-thrust representation to rudder drag may suffice.

$$X \text{ (rudder)} = k_{x,\delta} \rho d^4 n^2 \delta^2 \qquad (9)$$

Here we express $k_{x,\delta} = a_3 + a_4 s$, leading to

$$X \text{ (rudder)} = [(\rho d^4 a_3) n^2 + (\rho d^3 a_4) un] \delta^2 \qquad (10)$$

When the propeller is dragging or reversed, the rudder drag is small and erratic. No attempt is made to represent it.

Y Force Due to Propeller and Rudder

Representations of Y force and N moment due to propeller and rudder closely follow those for X force. The following will pertain to both Y and N.

Because the flow past the rudder (of a single-screw ship) is determined by both ship speed and propeller speed, the concept of k_t vs. J_s is useful for developing a polynomial representation for side force in the propeller operating region from 1 to 4 of Sketch I. If in this region Y is a linear function of rudder angle, the symmetrical part of Y (propeller + rudder) with respect to δ may be represented by

$$[(\rho d^4 b_o) n^2 + (\rho d^3 b_1) un + (\rho d^2 b_2) u^2] \delta$$

A small unsymmetrical side force is also observed for single-screw ships. This is called the Hovgaard effect[6] and is caused by asymmetry of propeller rotation. Several authors attempt to explain this physically, but it is represented here as a simple function of u and n, based on the results of straight-course experiments presented in the next section. Summing the symmetrical and unsymmetrical parts, the total expression is

$$Y \text{ (propeller + rudder)} = [(\rho d^4 b_o) n^2 + (\rho d^3 b_1) un + (\rho d^2 b_2) u^2] \delta + (\rho d^4 b_3) n^2 + (\rho d^3 b_4) u^2 \qquad (11)$$

In the stalled region, for advance ratios much to the right of point 4, flow aft of the propeller is much disturbed. Rudder forces are then sharply reduced and difficult to

evaluate. In this condition, it is estimated that rudder effectiveness is reduced to less than 1/3 of that in normal ahead operation. This is based on model tests of a related single-screw hull with propeller removed.[17]

As propeller rotation is reversed, the propeller race is directed forward. Local flow past the rudder is destroyed and steering control is lost. Side-force bias due to propeller rotation gains importance, and alone influences the directional behavior of the ship (in the absence of other external forces).*

N Moment Due to Propeller and Rudder

The representation of yaw moment produced by propeller and rudder, N (propeller + rudder), closely follows that for side force. An additional length dimension appears in the exponent of d. The number of terms in J_s will depend upon the shape of the function k_N, and the precision required.

A summary of terms used in the present study for N (propeller + rudder) appears below:

Operating Region of Propeller	Expression for Rudder-Propeller Yaw Moment	
1 to 4	$N_{\delta,n} = (\rho d^5 c_0 n^2 + \rho d^4 c_1 un + \rho d^3 c_2 u^2)\delta + \rho d^6 c_3 n^2$	(12)
4 to 6	$N_{\delta,n} = \rho d^3 c_4 u^2 \delta$	(13)
6 to 8	$N_{\delta,n} = \rho d^5 c_5 n^2$	(14)

TIME LAGS OF PROPELLER AND RUDDER RESPONSE

Engine Orders

Commands from the bridge to engine-control indicate desired magnitude and sense of propeller rotation.** A typical engine-order (bell) table for a merchant ship is shown:

Engine Order	Propeller Speed (rpm)
Full Ahead	60
Half Ahead	40
Slow Ahead	20
Dead Slow Ahead	10
Stop	0
Slow Astern	-15
Half Astern	-30
Full Astern	-45

*Although insufficient data are available to analyze ship dynamic stability in this condition, the reversed propeller may destabilize the ship by its effect on the flow about the hull. While this could cause yaw divergence in either direction, at low speeds the unbalanced side force produced by the reversed propeller usually causes yaw angle to develop in the positive (clockwise) sense. This tendency is shown in later computations. The yaw effect is used to advantage by ship-handlers and explains their preference for port-side-to-pier landings.

**Bridge control is not treated here, but may be introduced immediately since there is no restriction to discrete propeller speeds in this analysis.

The system used aboard naval ships is slightly different. In the naval system, the engine (propeller) is specified, followed by the desired sense and speed of rotation (in thirds). For this study a merchant ship is assumed.

Engine response to orders requiring large amounts of power is limited by the steam pressure available. Minimum allowed levels are established to protect the boiler against excess steam drain through the astern turbine. These limits guide throttle opening until desired propeller speed is approached.

Propeller Time Lag

Rate of change of propeller speed will depend upon —

1. Instantaneous propeller speed, n
2. Instantaneous ship speed, u
3. Previous steady propeller speed, n_i , and nozzle combination
4. Propeller speed ordered, n^*

A complete analysis of transient propeller speed would require propulsion-machinery characteristics and human-response factors beyond the scope of the present study. A simplified function is used, which provides a good approximation for the purposes of this work. It is based on full-scale ship data for the "crashback" maneuver.[19] Propeller response is described by the first-order differential equation $dn/dt + c_1 n + c_2 = 0$. Applying boundary conditions $n = n_i$ at $t = t_i$ and $n \to n^*$ as $t \to \infty$, instantaneous propeller speed is given by

$$n = n_i + (n^* - n_i)\ (1 - e^{-\Delta t/T}) \ , \ \Delta t = t - t_i \qquad (15)$$

where T = time constant for particular ship and maneuver. This may be estimated by fitting Equation (15) to given response data.

Rudder Time Lag

The steering machinery of a large ship will provide approximately constant rudder rotation for rudder changes of more than a few degrees. According to U. S. Coast Guard Marine Engineering Regulations and American Bureau of Shipping Rules, average rudder rotation shall not be less than about 2-1/3 degrees per second. In the S.S. GOPHER MARINER trials,[20] the rudder was shifted from 35 degrees left to 35 degrees right in 22 seconds, i.e., at an average rate of 3.2 degrees per second.

For constant rudder angular rate, rudder deflection is represented by $\delta = \delta_i + \dot{\delta}(t-t_i)$, and $\delta \gtrless \delta^*$ according to sense of rotation, where

δ_i = initial deflection angle

t_i = time at execution

$\dot{\delta}$ = rudder angular rate

δ^* = ordered rudder angle

The sign of $\dot{\delta}$ is determined by the sign of $(\delta^* - \delta_i)$. Rudder-angle commands are specified in degrees right or left of amidship (- or + , respectively), but radian measure is used in equations.

SUMMARY OF MOTION EQUATIONS

The equations of motion are summarized below in a form for solution:

X EQUATION

$$(m - A_o)\dot{u} = A_1 uU + (m + A_2)rv \qquad \text{X(Hull)}$$

$$+ \begin{cases} A_3 n^2 + A_4 un + A_5 u^2 + (A_6 n^2 + A_7 un)\delta^2 & , \quad 1/J_s > g_1 \\ A_8 uU + A_9 u^2 \delta^2 & , \quad g_1 \geq 1/J_s > g_2 \\ A_{10} n^2 + A_{11} un & , \quad g_2 \geq 1/J_s > g_3 \\ A_{12} n^2 + A_{13} un + A_{14} u^2 + A_{15} u^3/n & , \quad g_3 \geq 1/J_s \end{cases} \qquad \text{X(Prop. + Rudder)}$$

Y EQUATION

$$(m - B_o)\dot{v} = \begin{cases} B_1 uv + (B_2 - m)ur + B_3 rv^2/u + B_4 r^2 v/u + B_5 r^3/u + B_6 v^3/u \\ \qquad \text{for} \quad \beta \leq \beta_L, \; r' \leq r'_L, \text{ and } u \geq u_L \\ B_7 vU + B_8 v|v| + (B_9 - m)ur \\ \qquad \text{for} \quad \beta > \beta_L \text{ or } r' > r'_L \text{ or } u < u_L \end{cases} \qquad \text{Y(Hull)}$$

$$+ \begin{cases} B_{10} n^2 + B_{11} u^2 + (B_{12} n^2 + B_{13} un + B_{14} u^2)\delta & , \quad 1/J_s > g_1 \\ B_{15} u^2 \delta & , \quad g_1 \geq 1/J_s > g_2 \\ B_{16} n^2 & , \quad g_2 \geq 1/J_s \end{cases} \qquad \text{Y(Prop. + Rudder)}$$

N EQUATION

$$(I_z - C_o)\dot{r} = \begin{cases} C_1 uv + C_2 ur + C_3 rv^2/u + C_4 r^2 v/u + C_5 r^3/u + C_6 v^3/u \\ \qquad \text{for} \quad \beta \leq \beta_L, \; r' \leq r'_L, \text{ and } u \geq u_L \\ C_7 vu + C_8 vu|vu|/U^2 + C_9 r|r| \\ \qquad \text{for} \quad \beta > \beta_L \text{ or } r' \geq r'_L \text{ or } u < u_L \end{cases} \qquad \text{N(Hull)}$$

$$+ \begin{cases} C_{10} n^2 + (C_{11} n^2 + C_{12} un + C_{13} u^2)\delta & , \quad 1/J_s > g_1 \\ C_{14} u^2 \delta & , \quad g_1 \geq 1/J_s > g_2 \\ C_{15} n^2 & , \quad g_2 \geq 1/J_s \end{cases} \qquad \text{N(Prop. + Rudder)}$$

Equations (16)

and

$$n = n_i + (n^* - n_i)(1 - e^{-\Delta t/T}) \; ; \quad \Delta t = t - t_i \tag{17}$$

$$\delta = \delta_i + \dot{\delta}(t - t_i) \quad , \quad -\delta_L \leq \delta \leq \delta_L \tag{18}$$

where

$$A_o = \frac{\rho}{2} L^2 HX_u' \qquad B_o = \frac{\rho}{2} L^2 HY_v' \qquad C_o = \frac{\rho}{2} L^4 HN_r'$$

$$A_1 = \frac{\rho}{2} LHX_o' \qquad B_1 = \frac{\rho}{2} LHY_v' \qquad C_1 = \frac{\rho}{2} L^2 HN_v'$$

$$A_2 = \frac{\rho}{2} L^2 HX_{rv}' \qquad B_2 = \frac{\rho}{2} L^2 HY_r' \qquad C_2 = \frac{\rho}{2} L^3 HN_r'$$

$$A_3 = \rho d^4 a_o \qquad B_3 = \frac{\rho}{4} L^2 H(Y_{rvv}' + Y_r') \qquad C_3 = \frac{\rho}{4} L^3 H(N_{rvv}' + N_r')$$

$$A_4 = \rho d^3 a_1 \qquad B_4 = \frac{\rho}{4} L^3 HY_{rrv}' \qquad C_4 = \frac{\rho}{4} L^4 HN_{rrv}'$$

$$A_5 = \rho d^2 a_2 \qquad B_5 = \frac{\rho}{12} L^4 HY_{rrr}' \qquad C_5 = \frac{\rho}{12} L^5 HN_{rrr}'$$

$$A_6 = \rho d^4 a_3 \qquad B_6 = \frac{\rho}{12} LH(Y_{vvv}' + 3Y_v') \qquad C_6 = \frac{\rho}{12} L^2 H(N_{vvv}' + 3N_v')$$

$$A_7 = \rho d^3 a_4 \qquad B_7 = \frac{\rho}{2} LHY_1 \qquad C_7 = \frac{\rho}{2} L^2 HN_1$$

$$A_8 = \rho d^2 a_5 \qquad B_8 = \frac{\rho}{2} LHY_2 \qquad C_8 = \frac{\rho}{2} L^2 HN_2$$

$$A_9 = \frac{\rho}{2} LH a_6 \qquad B_9 = \frac{\rho}{2} L^2 HY_3 \text{(inertial only)} \qquad C_9 = \frac{\rho}{2} L^4 HN_3$$

$$A_{10} = \rho d^4 a_7 \qquad B_{10} = \rho d^4 b_o \qquad C_{10} = \rho d^5 c_o$$

$$A_{11} = \rho d^3 a_8 \qquad B_{11} = \rho d^2 b_1 \qquad C_{11} = \rho d^5 c_1$$

$$A_{12} = \rho d^4 a_9 \qquad B_{12} = \rho d^4 b_2 \qquad C_{12} = \rho d^4 c_2$$

$$A_{13} = \rho d^3 a_{10} \qquad B_{13} = \rho d^3 b_3 \qquad C_{13} = \rho d^3 c_3$$

$$A_{14} = \rho d^2 a_{11} \qquad B_{14} = \rho d^2 b_4 \qquad C_{14} = \frac{\rho}{2} L^2 Hc_4$$

$$A_{15} = \rho d \; a_{12} \qquad B_{15} = \frac{\rho}{2} LHb_5 \qquad C_{15} = \rho d^5 c_5$$

$$B_{16} = \rho d^4 b_6$$

Ship motions, position and orientation relative to earth-fixed axes are provided by

$$\begin{aligned} u_o &= u\cos\psi - v\sin\psi + U_{c_o}\cos\psi_c \\ v_o &= u\sin\psi + v\cos\psi + U_{c_o}\sin\psi_c \\ r_o &= r \end{aligned} \tag{19}$$

$$\begin{aligned} x_o &= \int_o^t u_o dt + x_o(o) \\ y_o &= \int_o^t v_o dt + y_o(o) \\ \psi &= \int_o^t r dt + r(o) \end{aligned} \tag{20}$$

EXPERIMENTAL PROGRAM

Experiments were made to evaluate coefficients of the motion equations. The program was divided into three parts, according to the facilities used. Since the number and ranges of variables are extensive, test programs were limited to conditions necessary for application of the equations to particular maneuvers.

PROGRAM I: Straight-Course Experiment

A 14-foot captive model was towed at various speeds. Propeller speed was varied among positive and negative values, and rudder deflection was set at intervals between plus and minus 30 degrees. A Series 60 model was used, particulars of which are given in Table I (see Appendix D).

The propeller was driven by a frequency-controlled synchronous motor, integral with a propeller thrust and torque dynamometer. The power source and speed controller were located ashore and were connected electrically to the model through overhead cables via the towing carriage.

Rudder deflections were set manually, by use of a tiller and protractor.

The three force components measured were the longitudinal component X (in line with the model's longitudinal centerline) and the two lateral components Y_A and Y_B (perpendicular to the model's centerline, forward and aft). The net side force is $Y = Y_A + Y_B$. The net yaw moment (acting about a vertical axis through the model CG) is determined by $N = Y_A \times \xi_A + Y_B \times \xi_B$, where ξ is the longitudinal separation between the model center-of-mass and the force-measuring balances ($\xi_A > 0$, $\xi_B < 0$).

The force balances are of the differential transformer type, capable of measuring two orthogonal force components and a moment component about a central axis. Balance locations and constraints are shown in Sketch III below. The model was constrained against surge, sway, and yaw motions but was permitted freedom to heave, pitch and roll.

SKETCH III

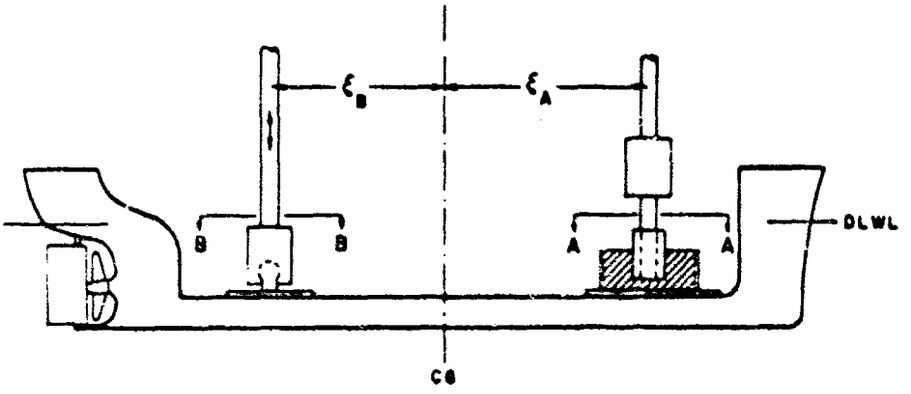

SECTION B-B

SECTION A-A

Tests in this program were conducted on straight path ($r' = 0$) with no drift angle ($v = 0$). Model speed, u, was varied between 0 and 5.7 feet per second. Propeller speed was varied between plus and minus 7.65 revolutions per second. No data are reported for propeller speeds less than 4.4 rps, for reasons of scale effect on forces. Rudder angles were limited to ±30 degrees, because of the effect of scale difference on the point at which rudder stall occurs (near 30 degrees).

Turbulence stimulation (of flow about the hull) was aided by a 0.03-inch-diameter trip wire located 8.4 inches aft of the forward perpendicular. It is unlikely that turbulent flow was achieved at most of the hull speeds of this test. However, hull resistance at low speeds is not significant compared with thrust forces. Furthermore, hull resistance is deducted from the total measured X-force in arriving at thrust coefficient information for use in ship-motion computations; thus, the error introduced is subsequently subtracted.

Hydrodynamic force and moment data are listed for various conditions of ship speed, propeller speed, and rudder angle (u, n, δ), in Table II (see Appendix D). These data are dimensional for the 14-foot-long model.

The data are reduced to coefficient form in Table III (Appendix D). The dimensionless coefficients are defined in the section on propeller and rudder forces or the section on hull forces. Apparent slip ratio, S_o, is given by

$$S_o = \frac{pn-u}{pn}$$

Coefficient data are plotted in Figures 2, 3 and 4, on the following pages.

PROGRAM II: Large-Drift-Angle Experiments

A 5-foot captive model was towed at various drift angles through a total range of 360 degrees. A Series 60 model was used, particulars of which are given in Table I (Appendix D). To avoid wall effects, the tests were conducted in Davidson Laboratory Tank No. 2, with the rotating arm at its longest practical radius. Side force and yaw moment were measured through the entire range of drift angles. Since coupling effects of propeller and rudder should be small relative to hull forces, they were neglected in the test. The propeller and rudder were both fixed.

The model was attached to the rotating arm in a manner similar to that used in conventional rotating-arm tests of surface-ship models.[18] The principal difference was that the flexure plate mounting on the model was made rotatable in steps of 90 degrees. This extended the drift-angle capability of the balance beyond the usual ±30-degree limits, to any desired angle. The normal arrangement, with fixed mounting, constrains the model against yaw, surge, sway, and roll motions, but permits freedom to pitch and heave. The modification changes the nature of the roll and pitch constraints; but only a negligible tendency to pitch or roll was detected at the low model speeds tested.

Model speed was selected according to the drift angle of the run. For drift angles near 0 or 180 degrees, speeds of between 1.5 and 2.5 feet per second were used. At large drift angles, the speed of 0.85 feet per second was used, to avoid unrealistically high Froude numbers in conditions that would exist only at very low ship speeds. Speed effect at 90-degree drift angle received special attention. The dimensionless side force coefficient

$$Y' = \frac{Y}{\frac{\rho}{2} LHU^2}$$

is plotted against speed for this condition, in Figure 5 (on a following page).

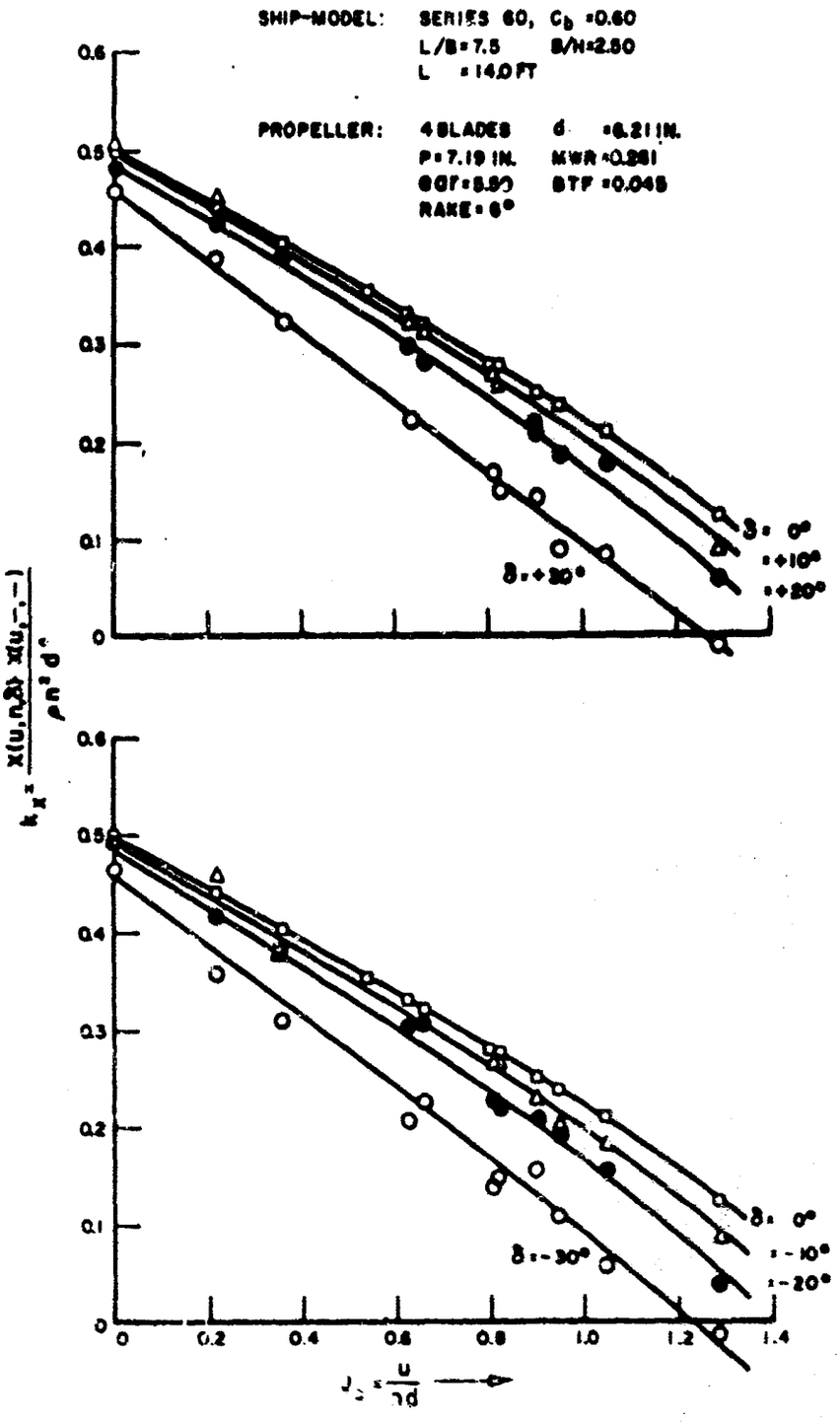

FIGURE 2. VARIATION OF LONGITUDINAL FORCE COEFFICIENT k_x WITH RUDDER ANGLE AND PROPELLER ADVANCE-RATIO IN BEHIND-SHIP CONDITION

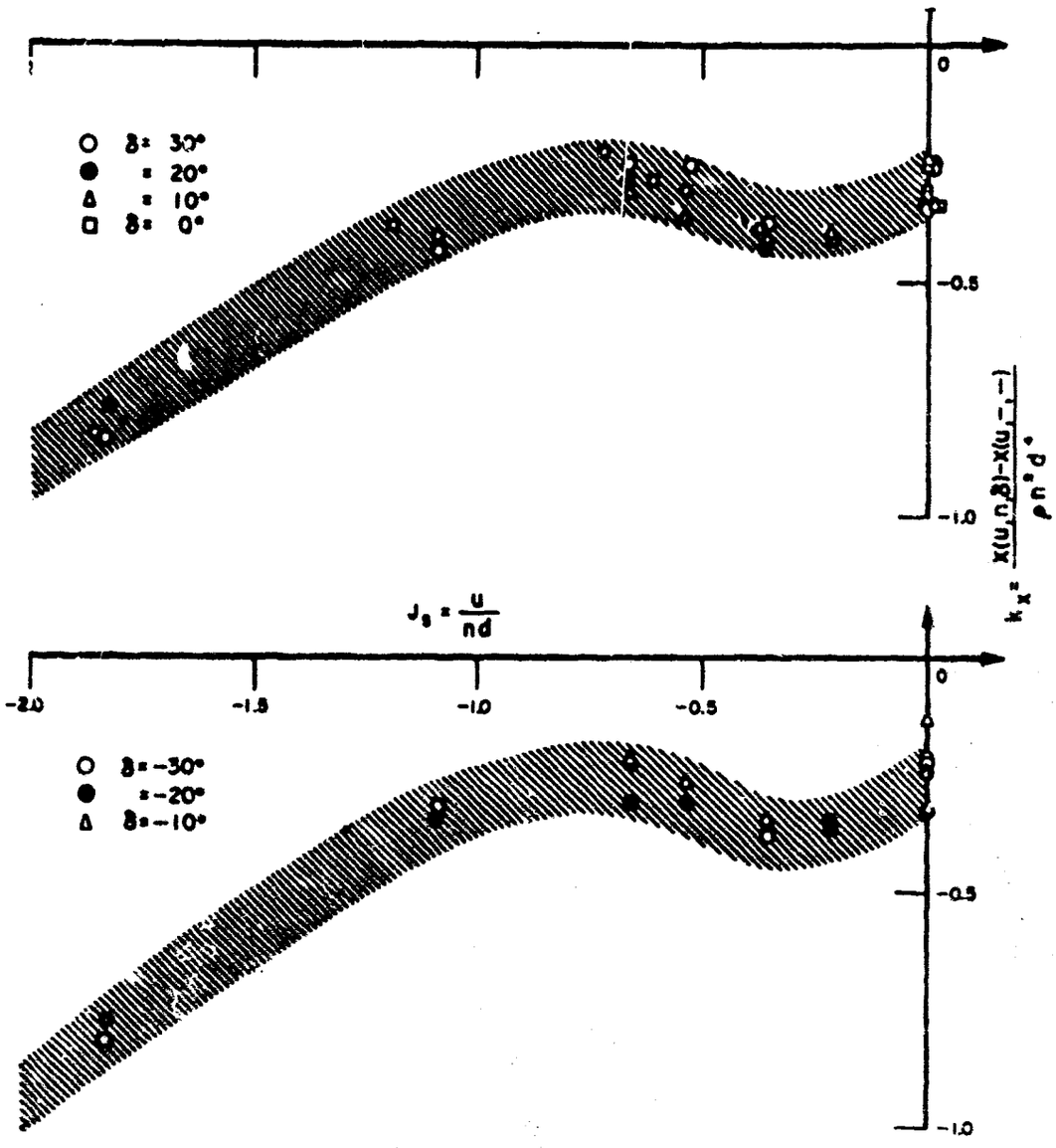

FIGURE 3. VARIATION OF LONGITUDINAL FORCE COEFFICIENT k_X, WITH RUDDER ANGLE AND ADVANCE RATIO OF PROPELLER IN BEHIND-SHIP CONDITION, $J_s = u/nd$ $(u > 0, n < 0)$

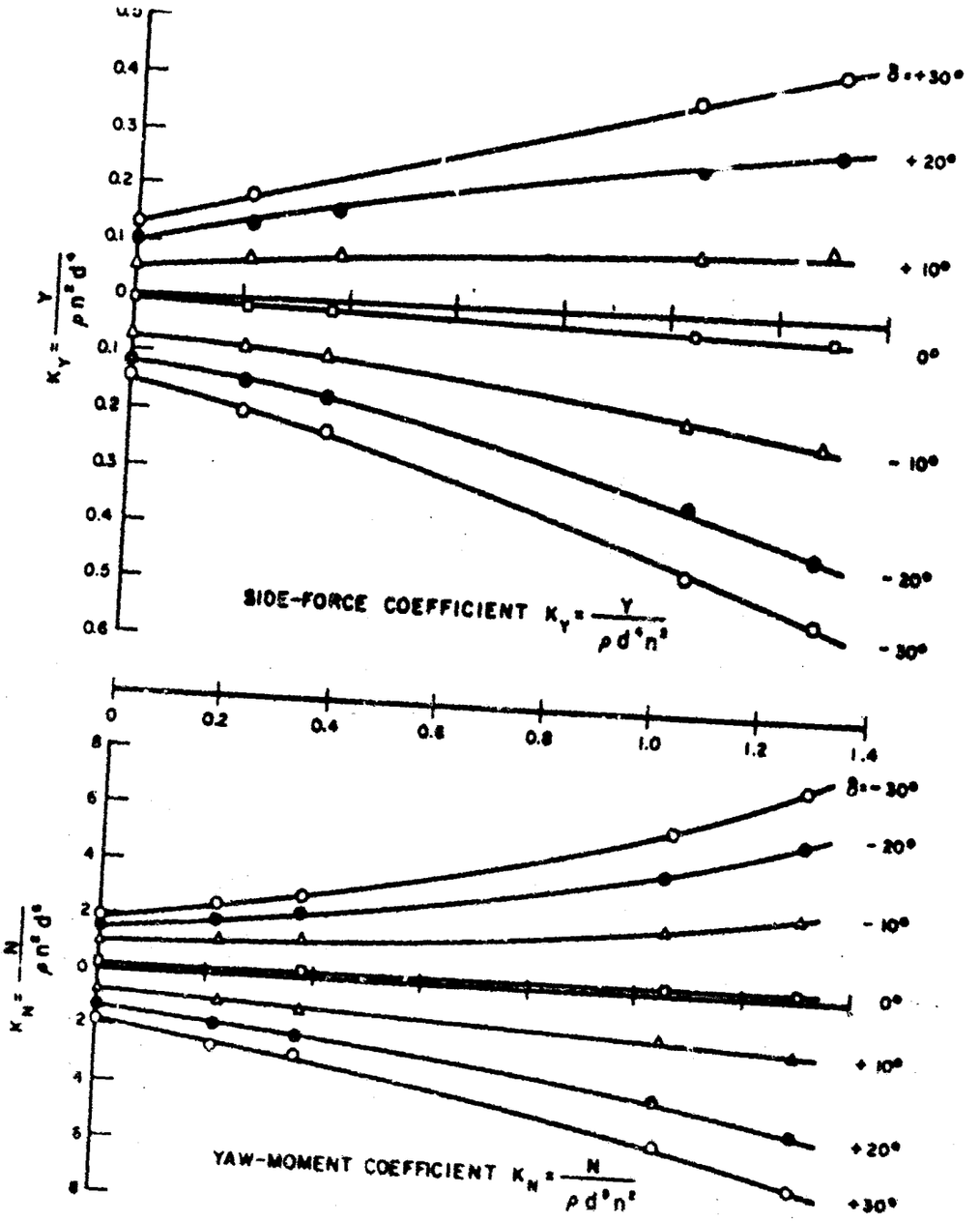

FIGURE 4. VARIATION OF SIDE-FORCE AND YAW-MOMENT COEFFICIENTS WITH RUDDER-ANGLE AND PROPELLER ADVANCE-RATIO IN BEHIND-SHIP CONDITION $J_s = \frac{u}{nd}$

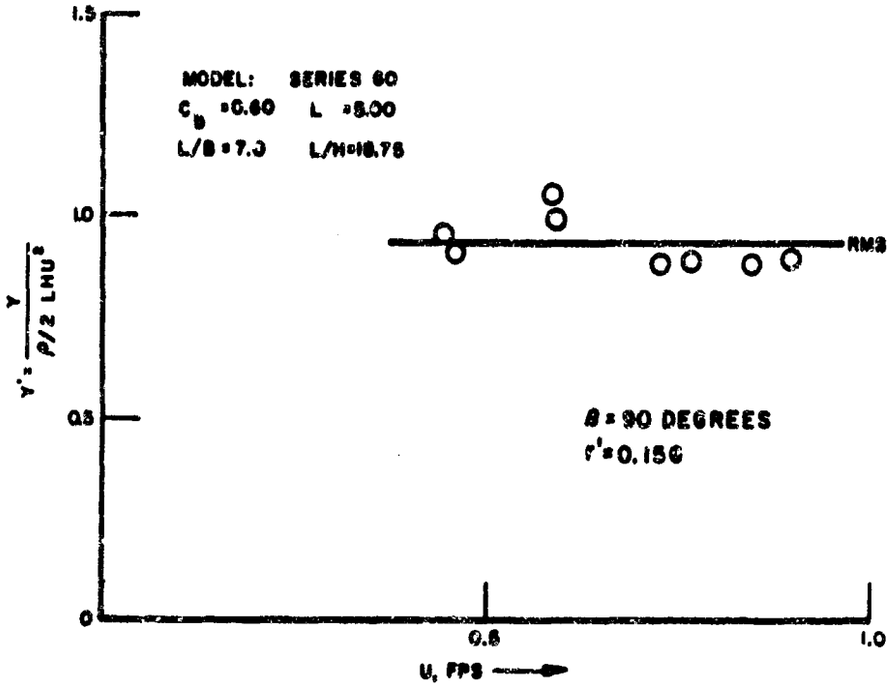

FIGURE 5. EFFECT OF MODEL SPEED ON SIDE-FORCE COEFFICIENT, Y'

Measurements comprised X and Y components of hydrodynamic force and N component of hydrodynamic moment. Dimensionless coefficients N', X', and Y' are formed, and plotted in Figures 6, 7, and 8, respectively (see immediately following pages). The rotating-arm facility imposed a small path curvature in all tests of this program. This effect was suppressed by averaging data taken at positive and negative drift angles. Averaged data are represented in the figures. In view of the symmetry of the averaged data, drift-angle arguments in the figures are shown only from 0 to 180 degress. Ideally, the drift-angle experiment would be conducted on straight course at many combinations of path curvature and drift angle.

PROGRAM III: Pure-Yaw-Rotation Experiment

A 5-foot model was torqued in pure yaw rotation by applying a known yaw moment via falling weights and pulleys. The resulting steady yaw rate was measured. A Series 60 model was used, particulars of which are given in Table I (Appendix D).

A vertical mast was erected in the model, coincident with the model's negative z-axis (through the CG). The mast was a drum having two fine cords attached, which, when wound around the drum, applied a pure yaw moment. The cords were led over ball-bearing pulleys attached to the outer sides of the walls of Tank No. 3. Weight holders were hung from the cords, and the system was arranged to permit the weights to hang freely and travel downward as the model commenced to rotate.

In testing, the lines were wound about the drum, elevating the weights. When the model had been positioned directly between the pulleys, it was released. After an acceleration interval, the time of one-half revolution in yaw was measured. Different weights permitted a determination of the effect of yaw rate on the dimensionless moment coefficient,

$$\frac{N}{\frac{\rho}{2} L^4 Hr^2}$$

Results are plotted in Figure 9. These show negligible change of coefficient value over the r range of the test.

COMPUTATION OF SIMPLE DOCKING MANEUVER

General

The equations of ship motion (16 through 20) were programmed for numerical integration by digital computer. The computer source program, written in Kingston Fortran language, is listed in Appendix B. The program applies to calculation of various turning, stopping, and accelerating maneuvers of a single-screw ship.

A representative application of the mathematical model is presented, in the calculation of a simple docking maneuver; namely, the "one bell" landing. This maneuver involves a single engine reversal for halting a ship alongside its berth. The particular purpose is to demonstrate sensitivity of ship response to operating and design parameters. Conditions of the maneuver are idealized in the sense that no tugboat or MPD forces are applied, no wind acts, and deep-water hydrodynamic coefficients are used. The one-bell landing is a legend for large ships, but as a limit maneuver it provides insight into the docking problem.

Characteristics of the study ship are given in Table I (Appendix D). Hull dimensions approximate the MARINER's, but are based on a Series 60 form. Coefficient values are listed in Table IV and values of other parameters in Table V (Appendix D). Conventional Y and N hydrodynamic derivatives are obtained from Reference 13 (Model 60).

To extend the results of computations to ships of other sizes, the following scaling laws may be used: Subscript A refers to the study ship, and B to a geometrically similar ship of different size. The factor λ is the scale ratio based on length; i.e., $\lambda = L_B/L_A$. Typical examples of scaling are shown below.

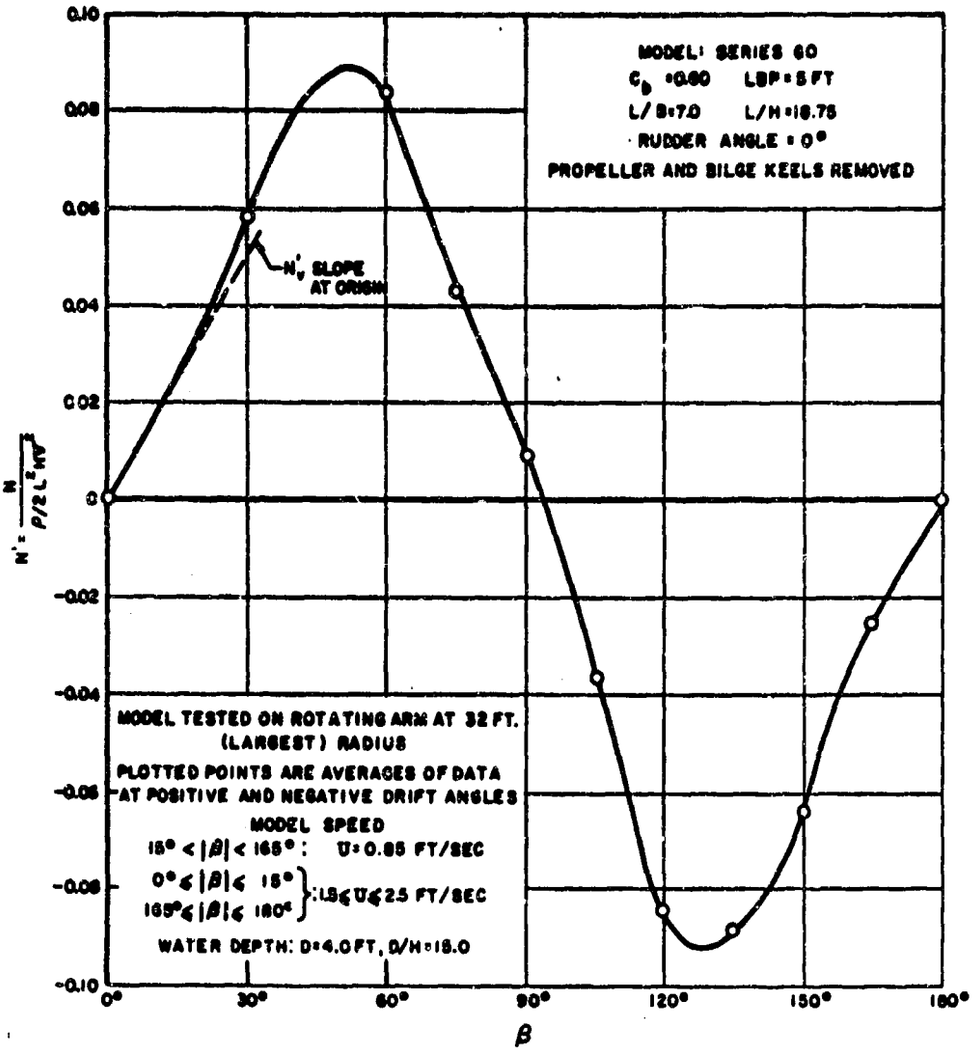

FIGURE 6. YAW MOMENT COEFFICIENT VERSUS DRIFT ANGLE
(MOMENT AXIS THROUGH MODEL C.G. – 0.015 L AFT OF [illegible])

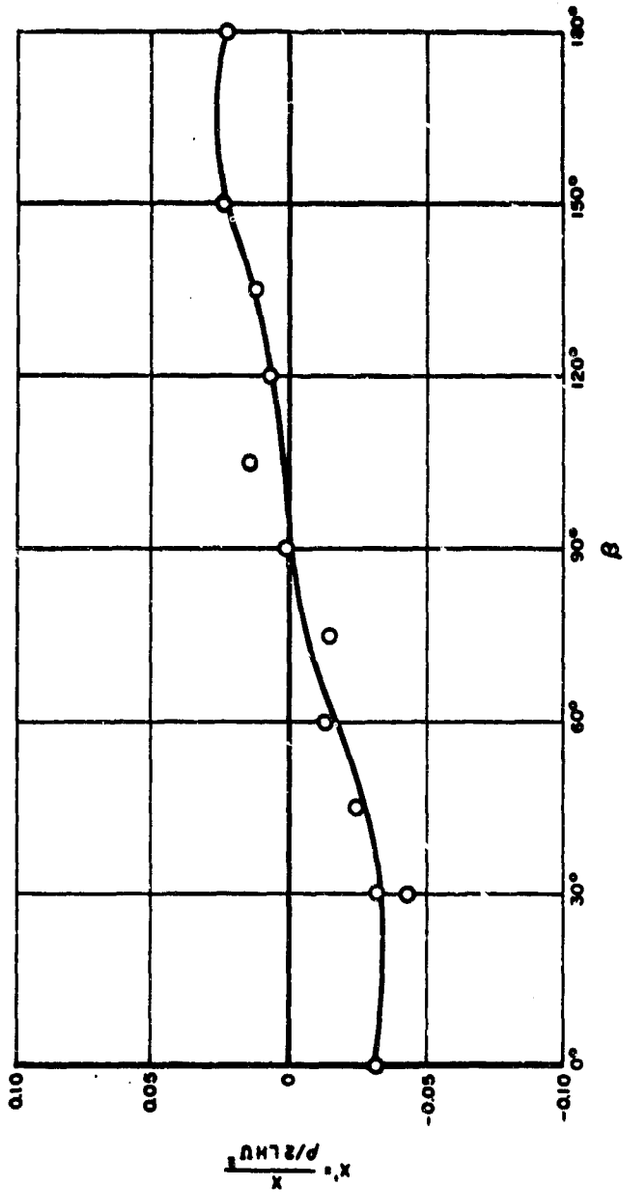

FIGURE 7. LONGITUDINAL FORCE COEFFICIENT VERSUS DRIFT ANGLE

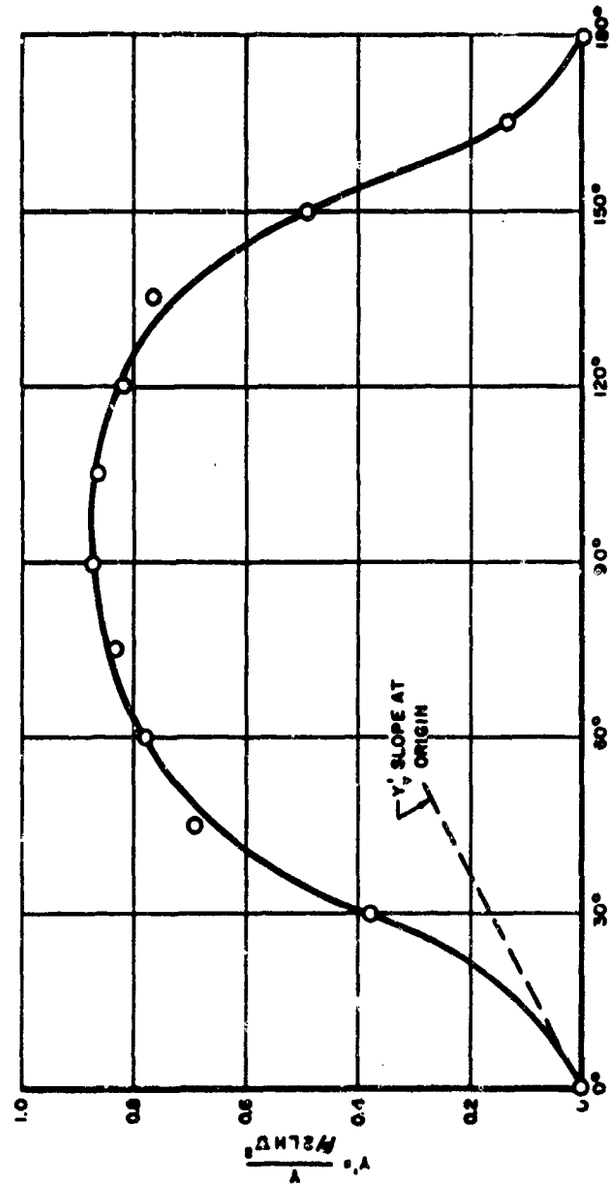

FIGURE 8. SIDE FORCE COEFFICIENT VERSUS DRIFT ANGLE

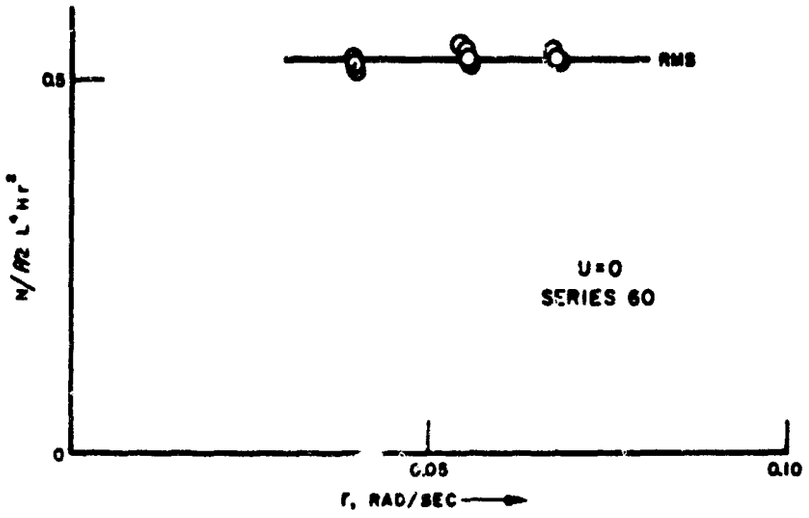

FIGURE 9. EFFECT OF MODEL ROTARY SPEED ON YAW MOMENT COEFFICIENT, $N/\rho/2\,L^4Hr^2$

Distance:	$x_B = x_A \times \lambda$	Linear acceleration:	$\dot{u}_B = \dot{u}_A \times 1$
Angle:	$\psi_B = \psi_A \times 1$	Angular acceleration:	$\dot{r}_B = \dot{r}_A \times \lambda^{-1}$
Time:	$t_b = t_A \times \lambda^{1/2}$	Speed(ship and current):	$u_B = u_A \times \lambda^{1/2}$
Force:	$X_B = X_A \times \lambda^3$	Angular speed:	$n = n \times \lambda^{-1/2}$
Moment:	$N_B = N_A \times \lambda^4$		

The correlation of hydrodynamic terms between models of different size (and especially between model and ship) is a major problem in ship hydrodynamics. For this reason a 14-foot-long model was used to measure forces depending on rudder actions, and friction scale effect was accounted for in scaling thrust forces. Still, the main interest of the work is to extend ship-motion analysis to permit evaluation of parameters affecting maneuvering performance at low speeds, and not the precise determination of ship response.

The basic conditions of the sample maneuver are these: The ship approaches a pier at a constant velocity of 4.3 knots, relative to the water. This corresponds to a propeller speed of 20 rpm. Turning rate and drift angle are initially zero. The "full astern" command is executed, and subsequent ship motions and trajectory are computed.

The calculation is repeated for several variations of each of the following parameters:

1. Maximum reversed propeller speed, n^*
2. Propeller-response time lag, i.e., time constant T
3. Velocity of uniform water current, $\bar{V}_{c_o}$

With propeller reversed at low ship speed, rudder deflection was found to have negligible effect on ship motion and trajectory; hence, it is not included as a parameter in these computations.

The distance and time required to stop are used as performance criteria for studying sensitivity to parameters 1 and 2. For parameter 3, the lateral trajectory characteristics, position and velocity, are used.

The computation proceeds from t_o, when the command n^* to propeller is given. Formally, the initial conditions of motion are $u = u(0)$, $v=r=\dot{u}=\dot{v}=\dot{r}=0$. Initial heading, $\psi(0)$, is arbitrary unless water current is specified. Coordinates $x_o(0)$ and $y_o(0)$ are also arbitrary. Typical computer output is shown in Appendix C.

Results

The effects of maximum reverse propeller speed are shown in Figure 10, following. Clearly, variations of n^* about the base value of -45 rpm cause significant variations in head-reach and time-to-stop. For the study ship, -45 rpm corresponds to normal "full astern." This is the command most likely to be used for killing headway of a fully loaded vessel. The response to emergency full-astern (taken as -60 rpm) is significantly quicker, and responses to lower values such as half-astern (-30 rpm) are unacceptably sluggish for docking. The curves representing time- and distance-to-stop are similar in character under these conditions. This is in accord with the simplified relations between constant retarding force, X, and the time and distance necessary to destroy kinetic energy. Energy and motion equations yield

$$s = -\frac{(m-X_{\dot{u}})u_o^2}{2X} \quad \text{and} \quad t = -\frac{(m-X_{\dot{u}})u_o}{X}$$

At low ship speeds, X is mainly determined by n^2; hence, both s and t are proportional to $1/n^2$.

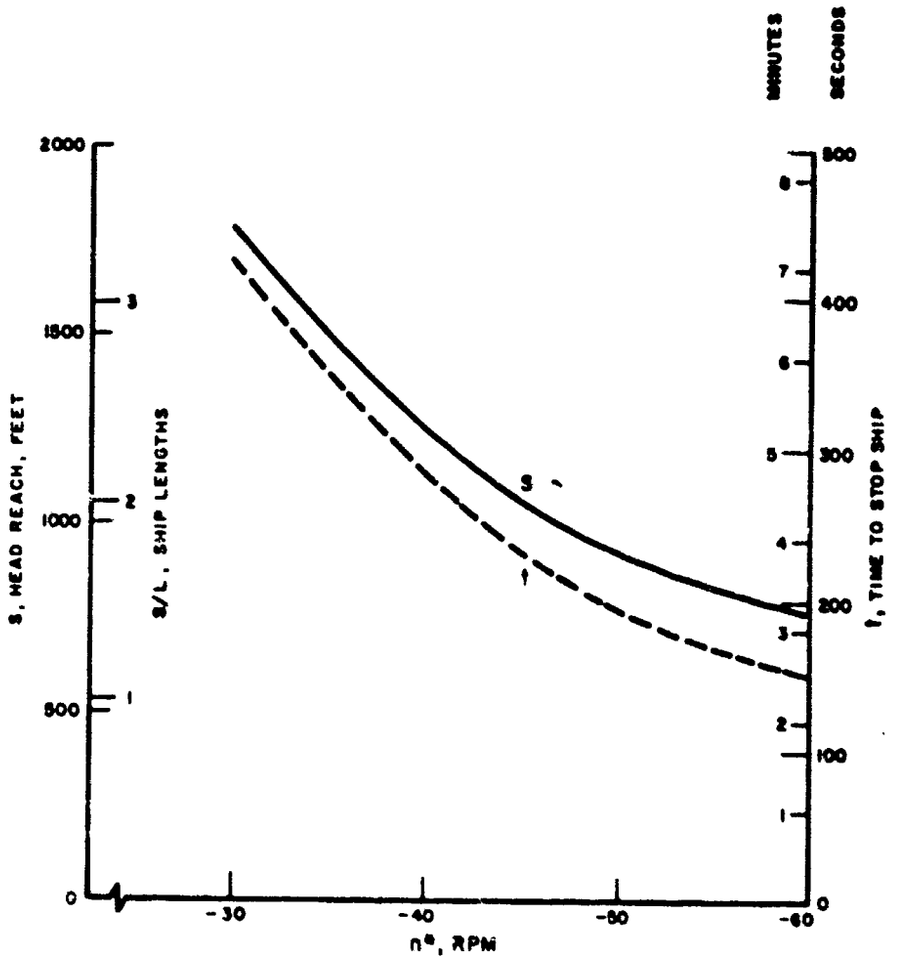

FIGURE 10. EFFECT OF REVERSED PROPELLER-SPEED ON DISTANCE AND TIME REQUIRED TO STOP SHIP FROM 4.3 KNOTS
(COMPUTATION OF SIMPLE DOCKING MANEUVER)

Figure 11 on the following page indicates how the response time of the engine affects distance- and time-to-stop. Since the time constant T is a measure of delay in achieving n^*, it dictates delay in reaching peak deceleration. This affects distance covered in each succeeding increment of time after t_o. Time-to-stop is not correspondingly affected, however.

The validity of the longitudinal ship-motion calculation was tested by computing stopping maneuvers of the ESSO SUEZ and comparing results with full-scale test data reported by Hewins, Chase, and Ruiz.[19]

Ship trajectories corresponding to three variations of the basic docking maneuver are pictured in Figure 12. Water current is the parameter. A time history of significant computational variables for the no-current condition is shown in Figure 13. Computed yaw-angle and drift-angle values develop significantly prior to ship stopping. Measurements of free maneuvering are unavailable for verification of these results, but tendencies appear to be correct in the light of experience with full-scale ships. The general preference of ship-handlers for port-side-to-pier landings is based on these effects (for right-hand single-screw ships).

Trial computations were carried out, to examine the importance of steady-state hydrodynamic terms in low-speed transient maneuvers. These computations showed that elimination of all steady-state hull terms did not appreciably affect the longitudinal motion results shown in Figure 13. However, effects on lateral motions were quite large, roughly doubling the values of yaw angle, drift angle, and lateral displacement. In another trial, only linear hull hydrodynamic terms were included. Results more in line with the basic computation were then obtained. However, it is cautioned that the simple docking maneuver does not involve large drift angle or space turning rate through most of the duration, as might be the case in other low-speed maneuvers.

The effect of uniform water current on a slowly moving ship is important. In Figure 12 the effect of a one-knot current, setting east, is compared with that of a one-knot current setting west (relative to a north-south pier). The right-hand ship is set heavily westward and put hard against the pier. The left-hand ship is set eastward, and a portside-to-pier landing is impossible. Therefore a starboard-side landing is shown. Because uniform water current adds a constant velocity to other ship motions, time-to-stop is very important in water-current cases.

A limiting criterion for docking is contact velocity with the pier. Lateral contact velocities of -2.3 feet per second* (for the ship set westward in Figure 12) or 1.1 feet per second (for the ship set eastward) could result in costly side-shell damage. A realistic non-uniform current would be weaker near the pier, and more confused, but the desirability of having additional lateral control forces available is apparent.

Dimensionless turning rate, r', is included in Figure 13. The r' variable corresponds to L/R in steady ship turning (with R the instantaneous turning radius); but this interpretation is lost in transient maneuvering. For example, in Figure 12 it is shown that ship trajectory may curve to the left as the ship yaws to the right. Dimensionless turning rate is, therefore, not suitable for discussing trajectory in transient maneuvers. In this study, r' is used only as a criterion of docking-type maneuvers.

CONCLUSIONS

The conclusions of this study are based on experimental results, results of computed maneuvers, and mathematical model development.

Conclusions Based on Experiments

1. Straight-course experiments show that the speed of an ahead-turning propeller strongly influences the rudder effectiveness of a single-screw ship. The relation may be

*Combined with yaw rotation, the lateral velocity at the stern (at station 18, on 20 stations) is -2.7 feet per second.

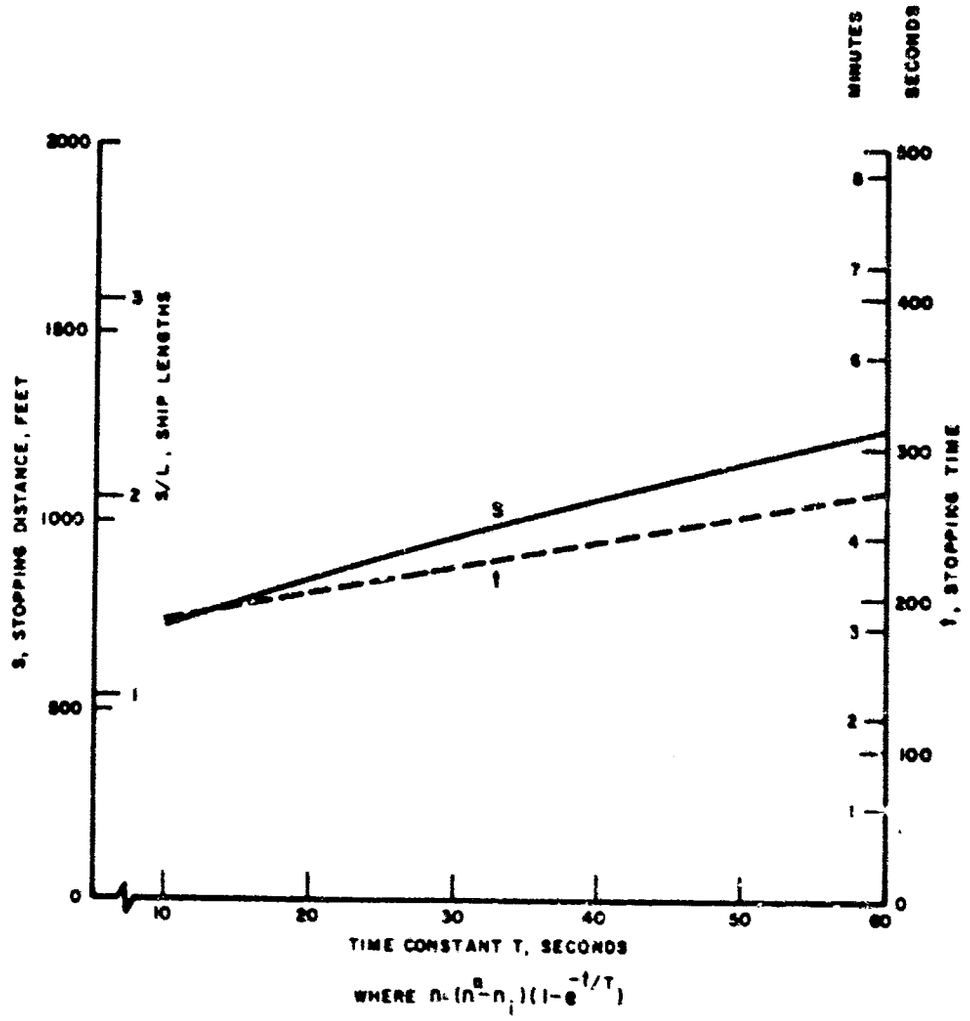

FIGURE II. EFFECT OF ENGINE-RESPONSE LAG ON DISTANCE AND TIME REQUIRED TO STOP SHIP FROM 4.3 KNOTS
(COMPUTATION OF SIMPLE DOCKING MANEUVER)

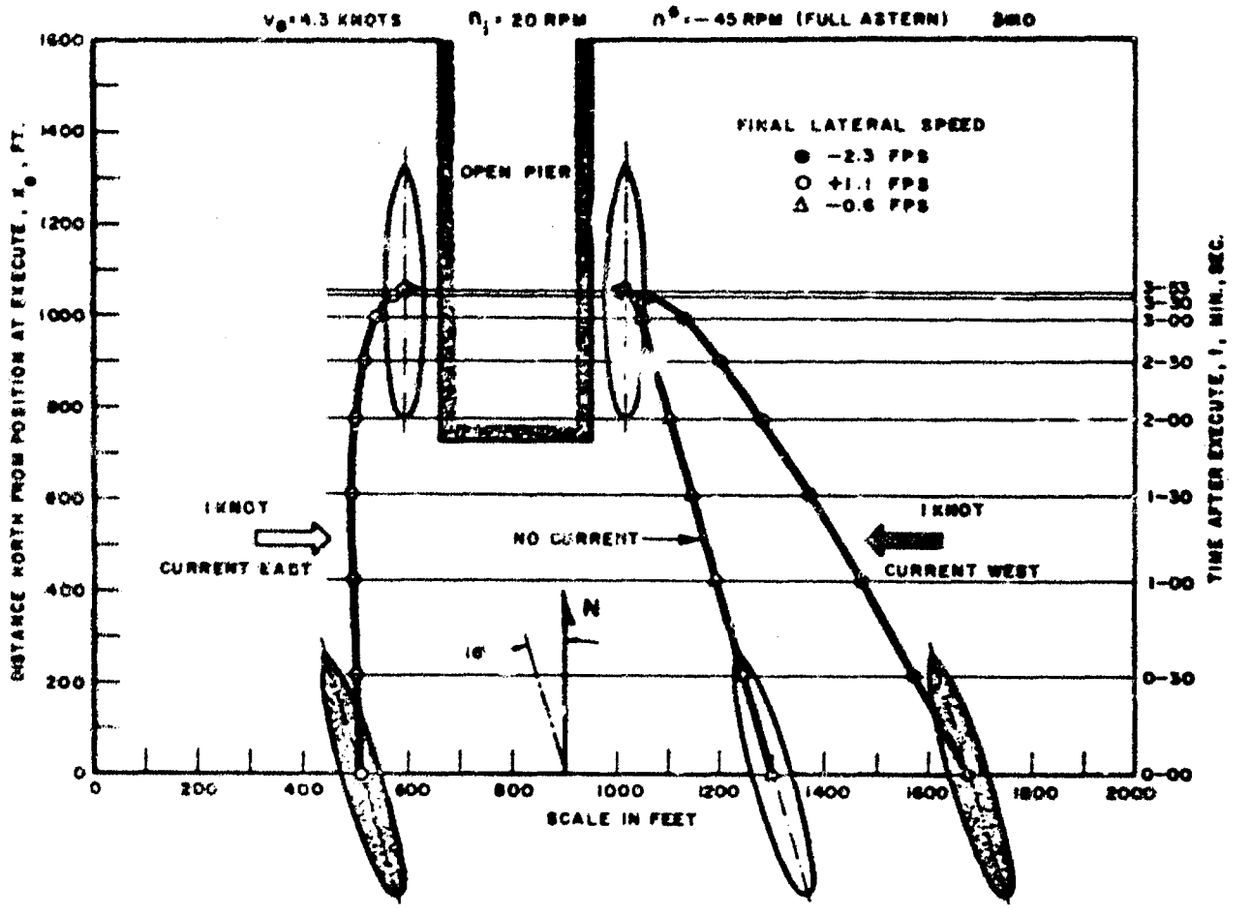

FIGURE 12. COMPUTED RESPONSE OF CARGO SHIP FOR SIMPLE "ONE BELL" LANDING

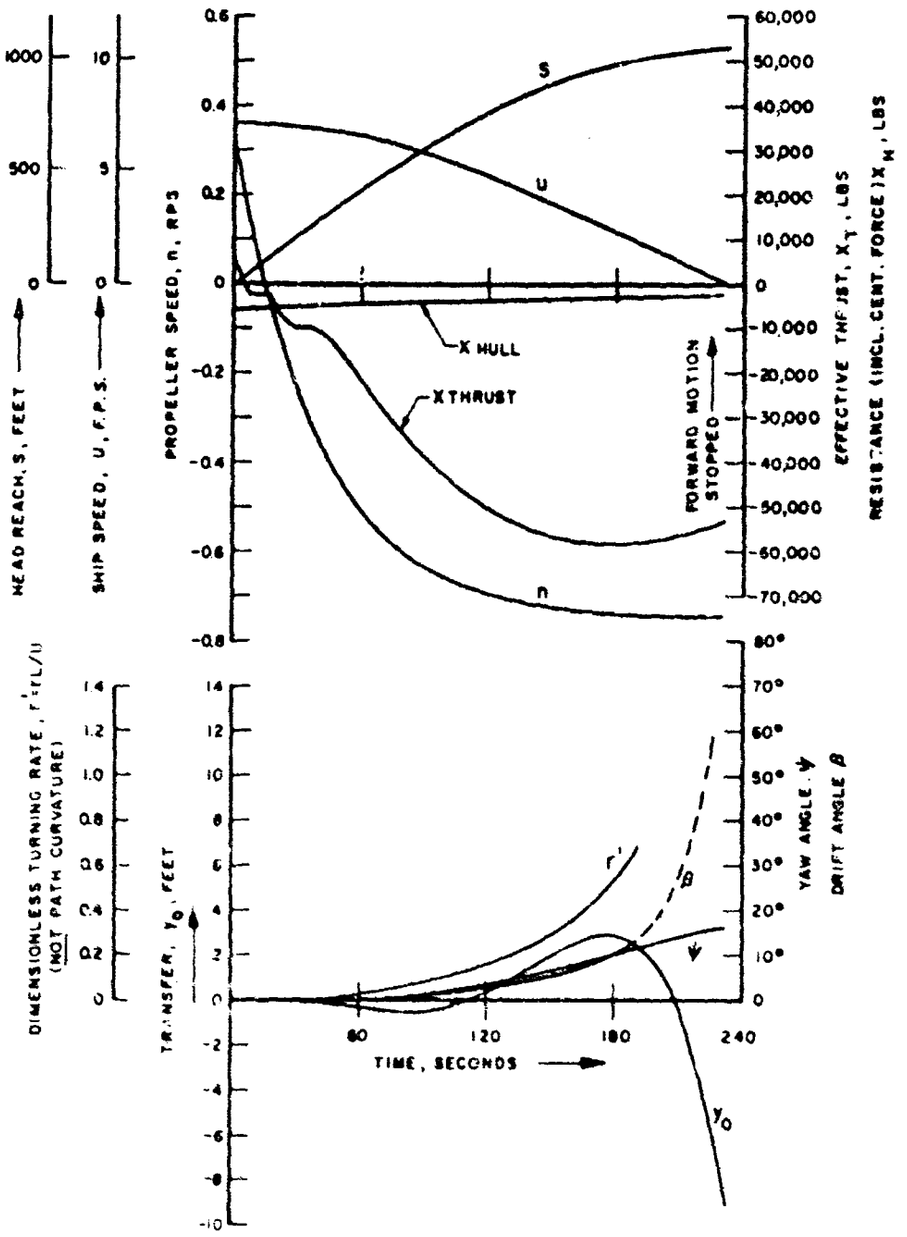

FIGURE 13. COMPUTED TIME-HISTORY OF PRINCIPAL VARIABLES IN TYPICAL DOCKING MANEUVER

expressed in terms of the propeller advance ratio J_s for ahead ship motions. When propeller rotation is reversed, rudder forces are small, erratic, and ineffective for control.

2. A significant side force is generated by the rotation of a single propeller behind a ship, especially for reversed propeller rotation at low ship speeds. This force is responsible for a tendency toward positive (clockwise) yaw rotation during ship-stopping. The ratio of measured yaw moment to side force locates the center of effort at approximately 10%L forward of the rudder post, for reverse propeller rotation, and approximately at the position of the rudder for ahead propeller rotation.

3. Hydrodynamic yaw moment resulting from pure yaw rotation is closely proportional to the square of yaw rate for a 5-foot Series 60 model at yaw rates between 0.04 and 0.07 sec^{-1}.

Conclusions Based on Computed Maneuvers

1. Computations show the importance of maximum reverse propeller speed, n^*, in ship-stopping from low speeds. Since hull resistance is minor at low speeds, the stopping force is mainly determined by n^* squared.

2. The time response of the engine importantly affects the speed with which astern thrust, hence ship deceleration, is established. Since this affects the time duration of the high-speed part of the maneuver, it has much greater effect on distance than on total time required to stop.

3. For some maneuvers, time-to-stop is more important than distance. For example, ship translation due to a uniform water current depends directly on total elapsed time, and not at all on distance traveled through the water. Therefore, a maneuver which may be simple for an unassisted ship in still water could be impossible in a modest current, depending on the time it takes to complete.

Conclusions Based on Development of Mathematical Model

1. Propeller forces are conveniently represented in motion equations by following the familiar k_t vs. J_s notation. Extension of the k_t, J_s concept assists in the representation of longitudinal force, lateral force, and yaw moment, as convenient functions of ship speed, propeller rotation, and rudder angle. Applied to both ahead and reverse propeller rotation, the technique provides insight into the changing propeller flow conditions. After blade stall, a locked propeller drag function may suffice until stall recovery. Computations may be organized on the basis of instantaneous J_s value.

2. If the water current can be assumed uniform, vector addition of ship motion through the water and motion of the water current permits a considerable simplification of the equations of motion. On the other hand, if water current is so irregular as to disallow this assumption, mathematical representation may be impractical.

3. In general, the variety of ship motions possible at low ship speed is boundless. Because of this, appropriate force and moment data are necessary in computations of low-speed ship maneuvers. Steady-state hydrodynamic reactions are complex functions which cannot be arbitrarily excluded from ship-motion equations, even at low ship speeds.

It is recommended that future experiments be designed to investigate a complete range of combinations of drift angle and space turning rate. Effects of shallow water should also be determined.

The mathematical model is a useful tool which may be extended to include additional forces, such as wind and auxiliary maneuvering devices. Constraints due to anchor or mooring lines may be added. With the proper data on external forces, the mathematical model provides an excellent means for analyzing many complex problems associated with low-speed ship maneuvers.

APPENDIX A

DRAG OF LOCKED PROPELLER

In the operating region between 4 and 6 of Sketch 1 (see section on "X Force Due to Propeller and Rudder"), the propeller force is essentially a drag force associated with propeller blades continuously changing orientation and angle of attack with respect to local flow. In the absence of detailed experimental data, a simple drag coefficient for a locked propeller can suffice. This may be estimated on the basis of developed blade area, DAR, ship speed, u, and mean wake fraction in way of the propeller, w.

$$X\,(\text{propeller})_{\text{dragging}} = C_D \frac{\rho}{2} A u_p^2$$

$$= C_D \frac{\rho}{2} \times DAR \frac{\pi d^2}{4} \times [u(1-w)]^2$$

$$= \rho d^2 a_s L^2$$

where

$$a_s = C_D \times DAR \times \frac{\pi}{8} \times (1-w)^2$$

Estimations of C_D for ship propellers are discussed in Reference 19.

APPENDIX B

COMPUTER PROGRAM FOR SIMPLE ENGINE-AND-RUDDER MANEUVERS

```
C       KINGSTON FORTRAN 2, 1620, STEVENS
        DIMENSION C(12,7)
    1   READ 100,((C(I,J),J=1,7),I=1,12)
        PUNCH 100
        PUNCH 101,((C(I,J),J=1,7),I=1,12)
        PUNCH 102
        CONL1=C(1,3)*C(1,4)*C(1,5)/2.0
        CONL2=CONL1*C(1,4)
        CONL3=CONL2*C(1,4)
        CONL4=CONL3*C(1,4)
        CONL5=CONL4*C(1,4)
        COND1=C(1,3)*C(1,6)
        COND2=COND1*C(1,6)
        COND3=COND2*C(1,6)
        COND4=COND3*C(1,6)
        COND5=COND4*C(1,6)
        A0=C(1,1)-CONL2*C(3,1)
        A1=CONL1*C(3,2)
        A2=C(1,1)+CONL2*C(3,3)
        A3=COND4*C(3,4)
        A4=COND3*C(3,5)
        A5=COND2*C(3,6)
        A6=COND4*C(3,7)
        A7=COND3*C(4,1)
        A8=COND2*C(4,2)
        A9=CONL1*C(4,3)
        A10=COND4*C(4,4)
        A11=COND3*C(4,5)
        A12=COND2*C(4,6)
        A13=COND1*C(4,7)
        A14=COND4*C(9,6)
        A15=COND3*C(9,7)
        B0=C(1,1)-CONL2*C(5,1)
        B1=CONL1*C(5,2)
        B2=CONL2*C(5,3)-C(1,1)
        B3=CONL2*C(5,4)
        B4=CONL3*C(5,5)
        B5=CONL1*C(5,6)
        B6=CONL4*C(5,7)
        B7=CONL1*C(6,1)
        B8=CONL1*C(6,2)
        B9=CONL2*C(6,3)-C(1,1)
        B10=COND4*C(6,4)
        B11=COND2*C(6,5)
        B12=COND4*C(6,6)
        B13=COND3*C(6,7)
        B14=COND2*C(7,1)
        B15=CONL1*C(7,2)
        B16=COND4*C(7,3)
        C0=C(1,2)-CONL4*C(7,4)
        C1=CONL2*C(7,5)
        C2=CONL3*C(7,6)
        C3=CONL3*C(7,7)
        C4=CONL4*C(8,1)
        C5=CONL2*C(8,2)
        C6=CONL5*C(8,3)
        C7=CONL2*C(8,4)
```

```
      C8=CONL2*C(8,5)
      C9=CONL4*C(8,6)
      C10=CONL5*C(8,7)
      C11=CONL6*C(9,1)
      C12=CONL4*C(9,2)
      C13=CONL3*C(9,3)
      C14=CONL2*C(9,4)
      C15=CONL5*C(9,5)
      YMPD=C(12,1)
      ENMPD=YMPD*C(12,2)*C(1,4)
      J=1
      T=C(11,5)
      U=C(10,1)
      V=C(10,2)
      UG=C(10,1)
      VG=C(10,2)
      R=C(10,3)
      RPSD=C(10,5)
      DEL=C(10,6)
      DELD=C(10,7)
      DELDOT=C(11,1)
      X=C(11,2)
      Y=C(11,3)
      S=C(2,7)
      PSI=C(11,4)
    7 W=SQRTF(U*U+V*V)
      RPRI=R*C(1,4)/W
      SRPRI=ABSF(RPRI)
      BETA=-ATANF(V/U)
      SBETA=ABSF(BETA)
      RPS=C(10,4)+(RPSD-C(10,4))*(1.0-EXPF(-(T-C(11,5))/C(1,7)))
      IF (SRPRI-C(2,2)) 50,50,51
   50 IF (SBETA-C(2,3)) 52,52,51
   52 IF (U-C(2,4)) 51,53,53
   53 XHULL=A1*U*W+A2*R*V
      YHULL=B1*U*V+B2*U*R+B3*R*V**2/U+B4*V*R**2/U+B5*V**3/U+B6*R**3/U
      ENHUL=C1*U*V+C2*U*R+C3*R*V**2/U+C4*V*R**2/U+C5*V**3/U+C6*R**3/U
      GO TO 3
   51 XHULL =A1*U*W+A2*R*V
      YHULL=B7*V*W+B8*V*ABSF(V)+B9*U*R
      ENHUL=C7*U*V+C8*V*U*ABSF(V*U)/W**2+C9*R*ABSF(R)
    3 RJ=RPS*C(1,6)/U
      IF (RJ-.376) 60,60,61
   60 IF (RJ+.158) 63,63,62
   63 IF (RJ+1.0) 65,65,64
   61 XCONN=A3*RPS**2+A4*U*RPS+A5*U**2+(A6*RPS**2+A7*U*RPS)*DEL**2
      YCONN=B10*RPS**2+B11*U**2+(B12*RPS**2+B13*U*RPS+B14*U**2)*DEL
      ENCON=C10*RPS**2+(C11*RPS**2+C12*U*RPS+C13*U**2)*DEL
      GO TO 4
   62 XCONN=A8*U*W+A9*U**2*DEL**2.
      YCONN=B15*U**2*DEL
      ENCON=C14*U**2*DEL
      GO TO 4
   64 XCONN=A14*RPS**2+A15*U*RPS
      YCONN=B16*RPS**2
      ENCON=C15*RPS**2
      GO TO 4
   65 XCONN=A10*RPS**2+A11*U*RPS+A12*U**2+A13*U**3/RPS
      YCONN=B16*RPS**2
      ENCON=C15*RPS**2
```

```
    4 UDOT=(YHULL+XCONN+C(2,5))/A0
      VDOT=(YHULL+YCONN+YMPD)/B0
      RDOT=(ENHUL+ENCON+ENMPD)/C0
      PDI=57.28*PSI
      BEDA=57.28*BETA
      DED=57.28*DEL
      ST=T*0.1
      JT=ST
      JT=JT*10
      JT=JT+1
      IF((JT/J)-1) 6,5,6
    5 PUNCH 103,T,PDI,U,X,Y,BEDA,RPRI,RPS,DLD,XCONN,XHULL,UDOT,UG,VG,S
    6 U=U+UDOT*C(2,1)
      V=V+VDOT*C(2,1)
      R=R+RDOT*C(2,1)
      PSI=PSI+R*C(2,1)
      UG=C(11,6)*COSF(C(11,7))+U*COSF(PSI)-V*SINF(PSI)
      VG=C(11,6)*SINF(C(11,7))+V*COSF(PSI)+U*SINF(PSI)
      X=X+UG*C(2,1)
      Y=Y+VG*C(2,1)
      S=S+W*C(2,1)
      IF(U-C(2,6)) 71,70,70
   70 IF (ABSF(DEL)-ABSF(DELD)) 40,41,41
   40 DEL=DEL+C(11,1)*C(2,1)
      GO TO 2
   41 DEL=DELD
    2 T=T+C(2,1)
      J=J+1
      GO TO 7
  100 FORMAT (55H
     1/(7E10.4))
  101 FORMAT(12(7E10.3/))
  102 FORMAT (42H    T       PSI    U          X          Y      BETA /66H1 RPRIME
     1 RPS    DELTA    THRUST    RESIST.  UDOT    UE      VE          S)
  103 FORMAT (F5.0,F7.1,F7.2,2F6.1,F7.2/1H1,2F7.3,F6.1,F10.0,F9.0,3F7.3,
     1F8.1)
   71 GO TO 1
      END
```

NOTE: Program allows inclusion of additional constant control forces in lateral and longitudinal directions, YMPD, NMPD, and XEX. These were made zero in the present study.

APPENDIX C

COMPUTER PRINT-OUT FOR DOCKING MANEUVER OF FIGURE 12

U_o = 4.3 kt n_i = 20 rpm n^* = -45 rpm δ_i = 0 δ^* = 0 U_{c_o} = 0 T = 40 sec

.135E+07	.235E+11	.199E+01	.529E+03	.282E+02	.195E+02	.400E+02
.107E+01	.100E+01	.262E+00	.845E+00	.000E+00	.100E+00	.000E+00
-.690E-02	-.750E-02	.168E+00	.494E+00	-.231E+00	-.430E-01	-.141E+00
-.322E+00	-.590E-01	.000E+00	-.325E+00	.500E+00	.150E+01	.100E+01
-.168E+00	-.305E+00	.896E-01	-.614E+00	-.115E+01	-.320E+01	.101E+00
-.305E+00	-.650E+00	-.620E-02	-.100E-01	-.326E-01	.294E+00	.397E+00
.120E+00	.127E-01	-.800E-01	-.107E-01	-.954E-01	-.701E-01	-.143E+01
-.127E+00	-.304E+00	-.608E-01	-.954E-01	-.169E+00	-.525E+00	.150E+00
-.385E+01	-.411E+01	-.262E+01	-.610E-02	.790E+00	.300E+00	.600E+00
.725E+01	.000E+00	.000E+00	.333E+00	-.750E+00	.000E+00	.000E+00
.000E+00	.000E+00	.000E+00	.000E+00	.000E+00	.000E+00	.000E+00

T	PSI	U	X	Y	BETA	RPRIME	RPS	DELTA	THRUST	RESIST.	UDOT	UE	VE	S
0.	.0	7.25	.0	.0	.00	.000	.333	.0	5916.	-5846.	.000	7.250	.000	.0
10.	.0	7.21	72.3	.0	.03	.001	.094	.0	-2332.	-5785.	-.006	7.212	-.004	72.4
20.	.0	7.15	144.1	-.1	.03	.001	-.093	.0	-5170.	-5689.	-.008	7.152	-.003	144.2
30.	.0	7.06	215.2	-.1	.05	.003	-.238	.0	-10036.	-5538.	-.011	7.056	-.004	215.4
40.	.1	6.94	285.1	-.2	.11	.008	-.351	.0	-10979.	-5361.	-.012	6.941	-.006	285.4
50.	.1	6.81	353.8	-.2	.23	.016	-.440	.0	-15526.	-5172.	-.015	6.810	-.010	354.2
60.	.2	6.64	421.0	-.3	.41	.028	-.508	.0	-21555.	-4952.	-.019	6.643	-.011	421.6
70.	.6	6.43	486.3	-.4	.64	.042	-.562	.0	-27839.	-4702.	-.023	6.435	-.009	487.2
80.	.9	6.18	549.3	-.5	.94	.059	-.603	.0	-33683.	-4438.	-.027	6.184	-.003	550.4
90.	1.4	5.89	609.6	-.5	1.30	.078	-.636	.0	-38864.	-4176.	-.031	5.896	.006	611.0
100.	1.9	5.57	666.8	-.3	1.73	.101	-.661	.0	-43338.	-3932.	-.034	5.575	.018	668.5
110.	2.6	5.22	720.7	-.1	2.24	.127	-.681	.0	-47135.	-3720.	-.036	5.226	.032	722.7
120.	3.4	4.85	770.9	.3	2.85	.158	-.696	.0	-50308.	-3548.	-.039	4.855	.044	773.3
130.	4.3	4.46	817.3	.8	3.57	.194	-.708	.0	-52910.	-3423.	-.040	4.464	.054	820.1
140.	5.3	4.05	859.8	1.4	4.43	.237	-.717	.0	-54986.	-3344.	-.042	4.058	.059	863.0
150.	6.4	3.62	898.0	1.9	5.47	.289	-.725	.0	-56570.	-3309.	-.043	3.640	.056	901.7
160.	7.5	3.19	932.1	2.4	6.75	.354	-.730	.0	-57686.	-3306.	-.044	3.213	.044	936.2
170.	8.8	2.75	961.9	2.8	8.36	.435	-.735	.0	-58350.	-3320.	-.044	2.782	.022	966.4
180.	10.2	2.31	987.3	2.8	10.45	.539	-.738	.0	-58569.	-3324.	-.044	2.350	-.011	992.2
190.	11.6	1.87	1008.4	2.5	13.25	.676	-.741	.0	-58354.	-3284.	-.044	1.919	-.056	1013.8
200.	12.9	1.43	1025.3	1.5	18.09	.756	-.743	.0	-57715.	-2918.	-.043	1.499	-.136	1031.1
210.	14.0	1.00	1038.1	-.4	26.95	.873	-.744	.0	-56674.	-2639.	-.042	1.095	-.251	1044.4
220.	15.1	.58	1046.8	-3.6	43.20	1.141	-.746	.0	-55253.	-2557.	-.041	.704	-.376	1054.1
230.	16.0	.17	1051.8	-8.1	73.32	1.420	-.747	.0	-53476.	-2525.	-.040	.327	-.510	1061.0

APPENDIX D

TABLE I MODEL AND SHIP CHARACTERISTICS

HULL	14-FT MODEL	5-FT MODEL	SHIP
Length, BP, L , ft	14.00	5.00	528.5
Breadth, B , ft	1.868	0.714	75.5
Draft, H , ft	0.747	0.267	28.2
Block Coefficient, C_b	0.60	0.60	0.60
L/B	7.50	7.0	7.0
L/H	18.75	18.75	18.75
Displacement, Δ	731 lb F.W.	35.6 lb F.W.	19,300 L.T.
L x H , sq ft	10.46	1.335	14,900
Lateral Area of Hull, sq ft	10.35	1.320	14,750
Mass of Model, M , slugs	22.75	1.11	1,345,000
LCG/L from FP	0.515	0.515	0.515
Radius of Gyration in Air, ft			132.1
RUDDER			
Area of Rudder, A_R, sq ft	0.167	0.021	238
A_R/LH	0.016	0.016	0.016
Aspect Ratio of Rudder	1.90	1.90	1.90
PROPELLER			
Troost - 4 blades			
Diameter, d , ft	0.518	0.198	19.54
Pitch, p , ft	0.599	0.187	22.50
p/d	1.15	0.95	1.15
Mean Width Ratio, MWR	0.261	-	0.261
Expanded Area Ratio, EAR	0.550	-	0.550
Blade Thickness Fraction, Btf	0.045	-	0.045
Rake, deg	6	-	6

TABLE II STRAIGHT-COURSE FORCE AND MOMENT DATA

RUN NO.	u fps	n rps	δ deg	X lb	Y lb	N lb-ft
103	.00	7.65	0	4.14	-.06	.50
101	.00	7.65	10	4.14	.61	-2.78
99	.00	7.65	20	3.94	.77	-5.58
097	.00	7.60	30	3.64	.99	-7.08
105	.00	7.65	-10	4.20	-.62	4.24
107	.00	7.65	-20	4.00	-.98	8.50
109	.00	7.65	-30	3.80	-1.17	7.78
71	.86	7.65	0	3.50	-.07	.45
90	.86	7.65	10	3.34	.61	-4.14
92	.86	7.65	20	3.33	1.06	-7.72
94	.85	7.65	30	3.[illegible]	1.48	-10.30
43	.54	4.61	30	.9[illegible]	.33	-2.84
72	.86	7.65	-10	3.64	-.70	4.73
78	.86	7.70	-20	3.33	-1.25	8.34
84	.86	7.67	-30	2.83	-1.69	10.56
44	.58	4.59	30	.89	.31	-2.90
64	.86	4.59	0	1.11	-.08	.29
58	.87	4.61	10	1.05	.25	-1.80
52	.88	4.55	20	1.01	.44	-3.02
50	.84	4.52	30	.81	.49	-3.91
45	.88	4.59	30	.89	.33	-3.17
79	.86	4.59	-20	1.01	-.49	3.81
85	.88	4.59	-30	.81	-.68	4.22
104	.00	-7.65	0	-2.75	-.52	3.44
102	.00	-7.65	10	-2.75	-.64	3.48
100	.00	-7.65	20	-2.73	-.66	3.96
98	.00	-7.65	30	-2.83	-.60	3.81
106	.00	-7.65	-10	-2.64	-.47	3.65
108	.00	-7.65	-20	-[illegible].63	-.64	3.19
110	.00	-7.65	-30	-2.61	-.38	4.32
70	.86	-7.65	0	-3.43	-.09	3.01
91	.86	-7.65	10	-3.33	-1.[illegible]3	4.62
93	.86	-7.65	20	-3.23	-.81	2.47
95	.85	-7.65	30	-3.43	-.88	3.98
77	.86	-7.66	-10	-3.03	-.3[illegible]	1.90
83	.86	-7.67	-20	-2.93	-.81	3.17
89	.86	-7.65	-30	-3.03	-.74	3.41
69	.86	-4.56	0	-1.21	-.25	1.25
63	.86	-4.59	10	-1.31	-.15	.88
57	.86	-4.52	20	-1.31	-.35	1.24
51	.85	-4.61	30	-1.21	-.37	1.17
76	.86	-4.59	-10	-1.11	-.35	1.53
82	.86	-4.62	-20	-1.21	-.13	.96
88	.86	-4.59	-30	-1.21	-.18	.85
152	4.20	7.66	0	-.81	-.04	.01
154	2.79	4.96	0	-.30	-.03	-.11
159	4.22	7.42	0	-1.11	-.30	.39
160	4.23	7.44	0	-.97	-.09	.45
165	4.23	7.42	0	-1.01	-.16	.23
151	4.20	7.35	0	-.91	-.03	.11
167	2.79	4.76	0	-.33	-.04	.23
155	5.65	7.54	0	-3.04	-.11	-.42
161	4.22	4.75	0	-2.32	-.15	-.14
15[illegible]	2.79	4.53	0	-.51	-.09	.05
156	5.65	4.41	0	-5.25	-.19	-.83
169	1.44	-4.49	0	-1.11	-.07	.10
168	2.79	-7.42	0	-2.71	-.23	.33
164	4.23	-7.47	0	-5.47	.23	-2.49
166	2.79	-4.51	0	-2.12	.01	-.53
163	4.23	-4.41	0	-4.55	-.09	-.10
158	5.65	-4.45	0	-8.69	-.26	.86

TABLE III STRAIGHT-COURSE DATA IN COEFFICIENT FORM

RUN NO.	J_S	K_X	K_Y	K_N	S_o	Y'	N'
103	.00	.508	-.01	.12	1.000		
101	.00	.508	.05	-.71	1.000		
99	.00	.483	.10	-1.32	1.000		
97	.00	.453	.12	-1.70	1.000		
105	.00	.516	-.08	1.01	1.000		
107	.00	.491	-.12	1.54	1.000		
109	.00	.466	-.14	1.84	1.000		
71	.22	.446	-.01	.11	.812	-.01	.00
90	.22	.447	.07	-.98	.812	.08	-.04
92	.22	.422	.13	-1.63	.812	.14	-.07
94	.21	.385	.18	-2.44	.815	.20	-.10
43	.23	.318	.11	-1.73	.804	.11	-.06
72	.22	.460	-.09	1.12	.812	-.09	.05
78	.22	.418	-.15	1.75	.813	-.17	.08
84	.22	.359	-.21	2.49	.813	-.23	.10
44	.27	.323	.11	-1.91	.753	.07	-.04
64	.36	.416	-.03	.19	.687	-.01	.00
58	.37	.393	.08	-1.18	.677	.03	-.02
52	.36	.389	.15	-2.03	.686	.06	-.03
50	.36	.363	.17	-2.66	.690	.07	-.04
45	.37	.272	.11	-2.09	.682	.04	-.03
79	.36	.384	-.17	2.38	.687	-.07	.03
85	.36	.313	-.23	2.78	.687	-.09	.01
104	.00	-.337	-.06	.82	1.000		
102	.00	-.337	-.08	.82	1.000		
100	.00	-.335	-.08	.94	1.000		
98	.00	-.347	-.07	.90	1.000		
106	.00	-.345	-.03	.87	1.000		
108	.00	-.322	-.08	.76	1.000		
110	.00	-.320	-.05	1.02	1.000		
70	-.22	-.408	-.09	.71	1.188	-.09	.03
91	-.22	-.396	-.15	1.10	1.188	-.16	.04
93	-.22	-.383	-.07	.54	1.188	-.08	.02
95	-.21	-.408	-.11	.94	1.185	-.12	.04
77	-.22	-.358	-.04	.45	1.187	-.05	.02
83	-.22	-.345	-.07	.75	1.187	-.08	.03
89	-.22	-.358	-.09	.81	1.188	-.10	.03
69	-.36	-.380	-.09	.83	1.315	-.03	.01
63	-.36	-.410	-.05	.58	1.313	-.02	.01
57	-.37	-.423	-.12	.84	1.316	-.05	.01
51	-.36	-.372	-.13	.76	1.308	-.05	.01
78	-.36	-.341	-.12	1.00	1.313	-.05	.01
82	-.36	-.371	-.04	.62	1.311	-.02	.01
88	-.36	-.378	-.06	.58	1.313	-.02	.01
152	1.08	.183	.00	.00	.085	.00	.00
154	1.08	.209	-.01	-.06	.062	.00	.00
159	1.10	.158	-.04	.10	.050	.00	.00
160	1.10	.176	-.01	.12	.050	.00	.00
165	1.10	.171	-.02	.06	.048	.00	.00
151	1.10	.185	.00	.03	.046	.00	.00
167	1.13	.228	-.01	.14	.021	.00	.00
155	1.45	.067	-.01	-.05	-.252	.00	.00
161	1.47	.000	-.05	-.09	-.486	.00	.00
153	1.49	.180	-.03	.03	-.028	.00	.00
156	2.22	-.218	-.06	-.36	-.920	.00	.00
169	-.62	-.289	-.03	.07	1.534	.00	.00
168	-.73	-.221	-.03	.08	1.828	.00	.00
164	-1.09	-.408	.03	-.62	1.945	.00	.00
166	-1.20	-.390	.00	-.36	2.034	.00	.00
163	-1.85	-.829	-.03	-.07	2.602	.00	.00
154	-2.45	-1.518	-.09	.61	3.122	.00	.00

TABLE IV

COEFFICIENT VALUES FOR SHIP IN SIMULATED MANEUVERS

X'_u	-.0068	Y_3	- .0062
X'_o	-.0075	b_o	- .010
X'_{vr}	.168	b_1	- .0326
a_o	.494	b_2	.294
a_1	-.231	b_3	.397
a_2	-.043	b_4	.12
a_3	-.141	b_5	.0127
a_4	-.322	b_6	- .080
a_5	-.059	N'_r	- .0107
a_6	—	N'_v	- .095
a_7	.300	N'_r	- .070
a_8	.600	$1/2(N'_{rvv} + N'_r)$	-1.43
a_9	-.325	$1/2\ N'_{rrv}$	- .127
a_{10}	.500	$1/6\ N'_{rrr}$	- .304
a_{11}	1.50	$1/6\ (N'_{vvv} + 3N'_v)$	- .061
a_{12}	1.00	N_1	- .095
Y'_v	-.168	N_2	- .169
Y'	-.305	N_3	- .525
Y'_r	.089	c_o	.15
$1/2(Y'_{rvv} + Y'_r)$	-.614	c_1	-3.85
$1/2\ Y'_{rrv}$	-1.15	c_2	-4.41
$1/6\ Y'_{rrr}$	-3.20	c_3	-2.62
$1/6(Y'_{vvv} + 3Y'_v)$	.101	c_4	- .0061
Y_1	-.305	c_5	.79
Y_2	-.65		

TABLE V

FIXED PARAMETERS IN EXAMPLE COMPUTATIONS

$r'_L = 1.000$

$\beta_L = .262\ (15^\circ)$

$u_L = .845$ fps

$g_1 = .376$

$g_2 = - .158$

$g_3 = -1.00$

$\Delta t = 1.0$ sec (iteration time)

NOMENCLATURE

The basic nomenclature follows that of SNAME Technical and Research Bulletin No. 1-5. Principal exceptions are the choice of typical dimensions used in forming dimensionless quantities, and the use of additional notation.

Three different right-handed, rectangular coordinate frames are used:

1. (x, y, z) are body axes with origin at the center of gravity, x directed toward the bow along the longitudinal centerline hull axis, y directed toward starboard, and z from deck to keel. The x,y plane is horizontal with the ship in static equilibrium.

2. (x_0, y_0, z_0) are fixed relative to the earth, with the x_0 and y_0 axes in a horizontal plane and z_0 directed downward. When yaw angle ψ is zero, the x_0 and y_0 axes are parallel to the x and y axes, respectively.

3. (x_1, y_1, z_1) are fixed relative to the body of water, which moves with a constant velocity relative to (x_0, y_0, z_0). This velocity is called the water current and is denoted $\vec{U}_c$. The x_1, y_1, and z_1 axes are always parallel to the x_0, y_0, and z_0 axes, respectively.

Unless otherwise noted, all dimensionless hydrodynamic (hull) derivatives are evaluated at zero angular velocity and acceleration, zero angles of sideslip and rudder, and propeller speed set for model self-propulsion point. Definitions of symbols used are listed below:

$A_0, A_1, \ldots, B_0, B_1, \ldots, C_0$, etc.	hydrodynamic force and moment coefficients used in motion equations, formed from products of dimensionless coefficients and dimensional quantities ρ, L, H; for example, $B_1 = \rho/2\ LHY_v'$
$a_0, a_1, \ldots, b_0, b_1, \ldots, c_0$, etc.	dimensionless coefficients used in representations of propeller and rudder forces
CG	center of gravity
c_x	a propeller thrust coefficient, useful for stalled propeller
d	propeller diameter
g_1, g_2, g_3	bounding values of $1/J_s$, distinguishing different regions of propeller operation; used for selecting relevant representation during computation
$\vec{F}$	vector sum of external forces acting on ship
H	ship draft
I	ship inertia tensor
I_z	moment of inertia of ship about z axis
J_s	propeller advance ratio in behind-ship condition
k_X, k_Y, k_N	functions used when obtaining propeller and rudder force and moment representations; dimensionless
L	ship length, between perpendiculars
m	mass of ship

$\dot{N}$	hydrodynamic moment component relative to z axis; yaw moment
N	vector sum of external moments acting on ship
n	propeller speed of rotation
p	propeller pitch
r	angular velocity component of ship axes in z direction
r'	dimensionless angular velocity; $r' = rL/U$
r_L'	limiting value of r' for cruising-type maneuvers
$\dot{r}$	angular acceleration component of ship axes in z direction
T	time constant for propeller speed response
t	time
S_o	apparent slip ratio of propeller
s	distance along trajectory
U	speed of CG relative to fluid
U_{c_o}	speed of water current relative to earth
u, v	velocity components of CG relative to fluid, measured in directions of x and y axes, respectively
u_I, v_I	velocity components of CG relative to fluid, measured in directions of x_o and y_o axes, respectively; (x_I, y_I) and (x_o, y_o) coordinate frames always parallel
u_o, v_o	velocity components of CG relative to earth, measured in directions of x_o and y_o axes, respectively
u_{c_o}, v_{c_o}	velocity components of water current relative to earth, measured in directions of x_o, y_o axes, respectively
$\dot{u}$, $\dot{v}$	acceleration components of CG in directions of x and y axes, respectively
X, Y	hydrodynamic force components relative to x and y axes, respectively, longitudinal and lateral forces
Y_v', N_v'	typical dimensionless first derivatives of a hydrodynamic force and moment with respect to a velocity component
Y_r', N_r'	typical dimensionless first derivatives of a hydrodynamic force and moment with respect to an angular velocity component
$Y_{\dot{v}}'$, $N_{\dot{v}}'$	typical dimensionless first derivatives of a hydrodynamic force and moment with respect to a linear acceleration component
$Y_{\dot{r}}'$, $N_{\dot{r}}'$	typical dimensionless first derivatives of a hydrodynamic force and moment with respect to an angular acceleration component
Y_{rvv}', N_{rvv}'	typical dimensionless third derivatives of a hydrodynamic force and moment with respect to an angular velocity component and a lateral velocity component

X, Y, N (Hull)	Sums of X, Y, N attributed to hull motions, respectively
X, Y, N (Propeller + rudder)	Sums of X, Y, N attributed to propeller and rudder actions
β	drift-angle; $\sin \beta = - v/U$
β_L	limiting drift angle for cruising-type maneuvers
δ	rudder deflection
ρ	mass density of water
Ψ	yaw angle, measured about z_o axis, relative to x_o axis
Ψ_c	direction of water-current flow, measured about z_o axis relative to x_o axis
$\vec{\omega}$	angular velocity of ship relative to (x_o, y_o, z_o) axes

Subscripts

o	referred to axes fixed with respect to earth; also initial time when used with t
i	previous steady value
$*$	desired or commanded value

ACKNOWLEDGMENTS

The author wishes to express his appreciation to members of the Davidson Laboratory staff who have assisted in the experiments, reported work and the preparation of the manuscript. He also acknowledges the cooperation of the Office of Naval Research and the David Taylor Model Basin for their support of the work

Computations were carried out at the Computer Center of Stevens Institute of Technology, which is partly supported by the National Science Foundation.

REFERENCES

1. Norrbin, N. H., "A Study of Course Keeping and Manoeuvring Performance," DTMB Report 1461, 1960.

2. Eda, H. and Crane, C. L., "Research on Ship Controllability - Part I, Survey and Long Range Program," DL Report 922, 1962.

3. Williams, V. E. and Noble, T. F., "Ships Bridge Control Console System," Sperry Piedmont Company Study Report, 1963 (not released).

4. Goodman, A., "Experimental Techniques and Methods of Analysis used in Submerged Body Research," Third Symposium on Naval Hydrodynamics, 1960.

5. Abkowitz, M. A., "Lectures on Ship Hydrodynamics - Steering and Maneouvrability," Hydro-Og Aerodynamisk Laboratorium, Lyngby, Denmark, May 1964.

6. Saunders, H. E., Hydrodynamics in Ship Design, Vol. III, SNAME, 1965.

7. Hawkins, S., "The Selection of Maneuvering Devices for Ships," Chesapeake Section of SNAME, September 1965.

8. Crane, C. L., Jr., Uram, E. M., and Chey, Y. H., "Equations of Motion for Mooring and Docking Maneuvers of a Destroyer and a Submarine," for U. S. Naval Training Devices Center (distribution temporarily limited), DL Report 1157, September 1966.

9. Crane, C. L., Jr., "Ship Stopping – A Study of Means to Improve Performance," DL Report (not yet released).

10. English, J. W., "The Design and Performance of Lateral Thrust Units for Ships," Trans. R.I.N.A., July 1963, Vol. 105, No. 3.

11. Stuntz, George R., Jr., and Taylor, R. J., "Some Aspects of Bow-Thruster Design," Trans. SNAME, 1964.

12. Strumpf, A., "Equations of Motion of Submerged Body with Varying Mass," DL Report 778, 1960.

13. Eda, H. and Crane, C. L., Jr., "Steering Characteristics of Ships in Calm Water and Waves," Trans. SNAME, 1965.

14. Lewis, F. M., "The Inertia of the Water Surrounding a Vibrating Ship," Trans. SNAME, 1929.

15. Prohaska, C. W., "The Vertical Vibration of Ships," Shipbuilder and Marine Engine Builder, October-November 1947.

16. Bindel, S. and Garguet, M., "Other Aspects of Propeller Action during Ship Stopping Maneuvers," Association Technique Maritime et Aeronautique, Session 1962.

17. Eda, H. and Crane, C. L., Jr., "Research on Ship Controllability - Part 2, Steering Characteristics of the Series 60 (C_b = 0.60)," DL Report 923, 1962.

18. Suarez, A., "Rotating-Arm Experimental Study of a Mariner-Class Vessel," DL Note 696 1963.

19. Hewins, E. F., Chase, H. J., and Ruiz, A. L., "The Backing Power of Geared-Turbine Driven Vessels," Trans. SNAME, 1950.

20. Russo, V. L. and Sullivan, E. K., "Design of the Mariner-Type Ship," Trans. SNAME, 1953.